ornl

NUREG/CR-4777
ORNL/TM-10272

OAK RIDGE
NATIONAL
LABORATORY

MARTIN MARIETTA

Steam Oxidation of Zircaloy Cladding in the ORNL Fission Product Release Tests

Toshiyuki Yamashita

Prepared for the
U.S. Nuclear Regulatory Commission
Office of Nuclear Regulatory Research
Under Interagency Agreement DOE 0551-0551-A1

PERATED BY
MARTIN MARIETTA ENERGY SYSTEMS, INC.
OR THE UNITED STATES
EPARTMENT OF ENERGY

Available from

Superintendent of Documents
U.S. Government Printing Office
Post Office Box 37082
Washington, D.C. 20013-7982

and

National Technical Information Service
Springfield, VA 22161

NUREG/CR-4777
ORNL/TM-10272
Dist. Category R3

Chemical Technology Division

STEAM OXIDATION OF ZIRCALOY CLADDING IN THE ORNL FISSION PRODUCT RELEASE TESTS

Toshiyuki Yamashita*

*Guest scientist from the Japan Atomic Energy Research Institute.

Manuscript Completed — February 1987
Date of Issue — March 1988

Prepared for the
U.S. Nuclear Regulatory Commission
Office of Nuclear Regulatory Research
Washington, DC 20555
under Interagency Agreement DOE 0551-0551-A1

NRC FIN No. B0127

Prepared by the
OAK RIDGE NATIONAL LABORATORY
Oak Ridge, Tennessee 37831
operated by
MARTIN MARIETTA ENERGY SYSTEMS, INC.
for the
U.S. DEPARTMENT OF ENERGY
under contract DE-AC05-840R21400

ABSTRACT

A simple model (ZIRCOX) has been developed to calculate the extent of oxidation of Zircaloy cladding in the vertical furnace tests conducted at ORNL. The model is based on the fact that the oxidation of Zircaloy is governed by the parabolic rate law. By introducing the equivalent time t^*, the model is able to handle nonisothermal oxidation as well as isothermal.

The degree of cladding oxidation and H_2 production were calculated using three sets of rate constants for the Zircaloy oxidation, and these results were compared with those measured experimentally. The calculated results showed excellent agreement with the experiments. The rate constant for Zircaloy oxidation that gave the best agreement was one based upon combined Pawel et al. and Prater and Courtright data.

The temperature difference between the cladding and the zirconia furnace tube liner was estimated by the HEATING6 heat transfer program and was found to be ~50 K for the maximum oxidation rate.

The heating atmosphere during test VI-1 was also evaluated in terms of the oxygen potential.

CONTENTS

LIST OF FIGURES

LIST OF TABLES

STEAM OXIDATION OF ZIRCALOY CLADDING IN THE ORNL FISSION PRODUCT RELEASE TESTS

Toshiyuki Yamashita

1. EXECUTIVE SUMMARY

The objectives of this report are (1) to describe the results of three tests that were performed to examine the oxidation of cladding and the resultant hydrogen production and (2) to present a description of the method that has been developed to evaluate the extent of oxidation of Zircaloy cladding in the vertical furnace tests. The comparison of the results obtained from the tests with the model calculations are also included.

In test VT-3, reported in Sect. 4.1, oxidation of Zircaloy cladding was performed in a steam-starved environment. The cladding was not oxidized uniformly: the degrees of oxidation of the top, middle, and bottom of the cladding were measured as 19, 44, and 75%, respectively. The overall oxidation of the cladding was measured as 53% based on the weight gain in the cladding specimen.

Tests VT-12 and VI-1 were conducted under highly oxidizing conditions. In those tests, the variation of the hydrogen and carbon monoxide (from graphite oxidation) production was measured as a function of run time in addition to a measurement of their total amounts. Results indicated that the oxidation of the cladding was completed in the second 20-min period, while the fuel temperature was kept at 2000 K.

The model for oxidation of Zircaloy cladding is described in Sect. 5. It has been developed to calculate the extent of oxidation of the cladding and resultant hydrogen production in the vertical furnace tests. The model is based upon the fact that the oxidation of Zircaloy is governed by the parabolic rate law. The important feature of this work is the introduction of the "equivalent time t^*" which makes it possible to easily handle the nonisothermal oxidation process as well as the isothermal one.

In Sect. 6, the calculated results are compared with those obtained from the experiments. The most important findings are:

1. By comparing the hydrogen production with that obtained experimentally, it was found that the rate constant for Zircaloy oxidation which gave the best estimation was one based upon combined Pawel et al. and Prater and Courtright data (the PPC data). The Urbanic and Heidrick data under-predicted the oxidation experiments at temperatures above ~1800 K, and the Baker and Just data over-predicted the Zircaloy/steam reaction in the temperature range between 1300 and 1800 K.

2. The oxidation model combined with the PPC data for the oxidation rate constant predicted the experimental data very well.

3. The best fitting profile of cladding oxidation in test VT-3 was obtained under conditions such that the steam supply rate was 0.55 L/min and the axial temperature gradient was ~75 K.

4. The temperature difference between the cladding and the surrounding zirconia furnace tube liner was evaluated by using the HEATING6 heat transfer computer program, because a large heat release from the Zircaloy/steam reaction could increase the surface temperature of the cladding. The results showed that the maximum temperature difference between the cladding and the surrounding zirconia liner was ~50 K.

5. The atmosphere during test VI-1 was estimated to be rich in steam. For most of the test, the H_2/H_2O ratio at the furnace outlet was <0.1 except for a short period in the run time between 49 and 54 min where the H_2/H_2O ratio was more than unity.

6. The oxygen potential of the atmosphere during the second and third 20-min periods of test VI-1 was evaluated to be in a range between -100 and -150 kJ/mol which was low enough to reduce oxides such as Cs_2O, TeO_2 and RuO_2 to their metallic states.

2. INTRODUCTION

Fission product release tests, which were sponsored by U.S. Nuclear Regulatory Commission (USNRC), have been conducted at Oak Ridge National Laboratory (ORNL) to clarify the release behavior of fission products from LWR fuel under severe fuel accident conditions and have provided experimental data for source term modeling.[1-11] The fission product release rates obtained in those tests were primarily correlated to the temperatures at which the tests were performed to yield equations of the form:

$$k = A\exp(-BT) \text{ or} \quad (1)$$

$$k' = A'\exp(-B'/T) , \quad (2)$$

where k is the fission product release rate coefficient; A, A', B, and B'are constants which are determined by experiments, and T is the absolute temperature.

However, there are several factors that affect fission product release other than the heating temperature. Three of the more important ones are (1) fuel burnup, (2) linear heat rating, and (3) the atmosphere surrounding the test fuel. The nature of the atmosphere is closely related to the oxidation of fuel cladding and varies considerably in the course of the experiment because of the change in the Zircaloy/steam reaction rate. Oxidation of the cladding and fuel affects fission product behavior in several ways:

1. Hydrogen, which is produced by the Zircaloy/steam reaction, affects the chemical form of the released fission products.

2. The amount of cladding oxidation affects the retention and release of tellurium.

3. Oxidation or reduction of the fuel by steam or Zircaloy can affect the release of fission products such as barium, strontium, molybdenum, and europium.

4. The extent of Zircaloy/UO_2 reaction (called liquefaction) is limited by the amount of unoxidized Zircaloy available.

5. The heat released during oxidation increases the cladding and fuel temperatures.

The main objective of this work was to develop a method for calculating the extent of oxidation of Zircaloy cladding in the vertical furnace tests so that the resulting chemical effects on fission product release, retention, and chemical form could be better understood. This report provides a description of the cladding oxidation tests, the cladding oxidation model in the vertical furnace assembly, and a comparison of the results obtained in the experiments with those obtained by calculations.

3. EXPERIMENTAL PROCEDURE

3.1 APPARATUS

A schematic diagram of the experimental apparatus which was used in the Zircaloy cladding oxidation tests is illustrated in Fig. 1. It consists of (1) a vertical furnace assembly, (2) fission product collection trains, and (3) an effluent gas analyzing system. A fuel specimen with a Zircaloy sheath was vertically positioned at the center of the zirconia furnace tube liner as shown in Fig. 2. A graphite tube surrounding the furnace tube liner was used as an induction coupling-susceptor to uniformly heat the clad fuel specimen. Temperatures of the furnace tube liner surface were measured at two different locations by use of a two-color optical pyrometer connected to an optical fiber and a disappearing filament-type optical pyrometer. A carrier gas mixture of helium and steam was supplied from the bottom of the furnace tube.

Details of the fission product collection trains and an effluent gas analyzing assembly are shown in Fig. 3. The effluent gas, which was a mixture of helium, steam, hydrogen, and carbon monoxide, was dried by an ice-bath-cooled condenser and a dry-ice-cooled freeze trap in the hot-cell cubicle. Hydrogen was formed in the furnace by the reactions of steam with the Zircaloy cladding of the fuel specimen and with the graphite susceptor. Carbon monoxide was also generated by the steam/graphite reaction. The barrier that restricts steam flow into the susceptor region has not been very effective. These reactions are described by the following chemical equations:

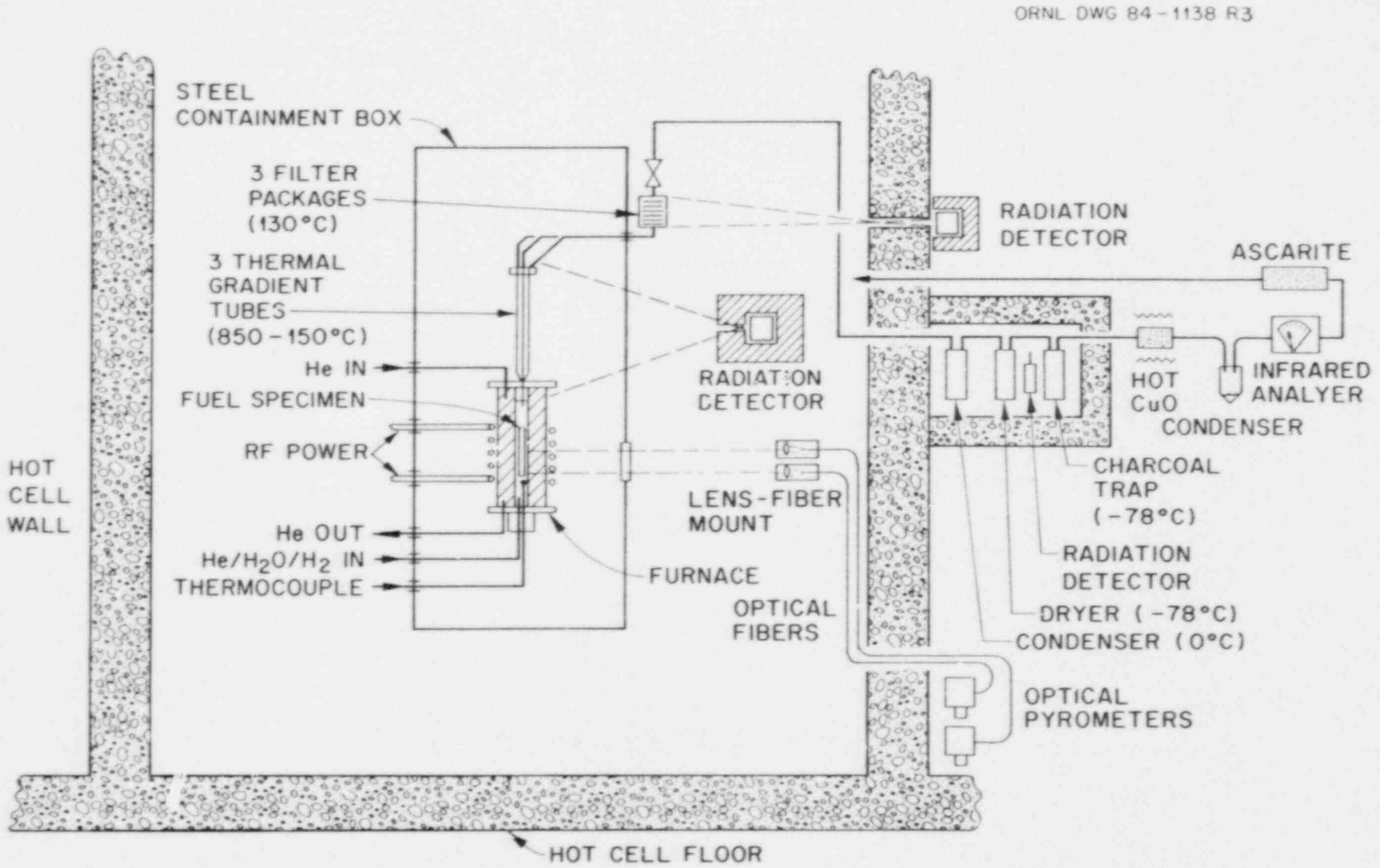

Fig. 1. Vertical fission product release apparatus.

ORNL DWG 85-496R2

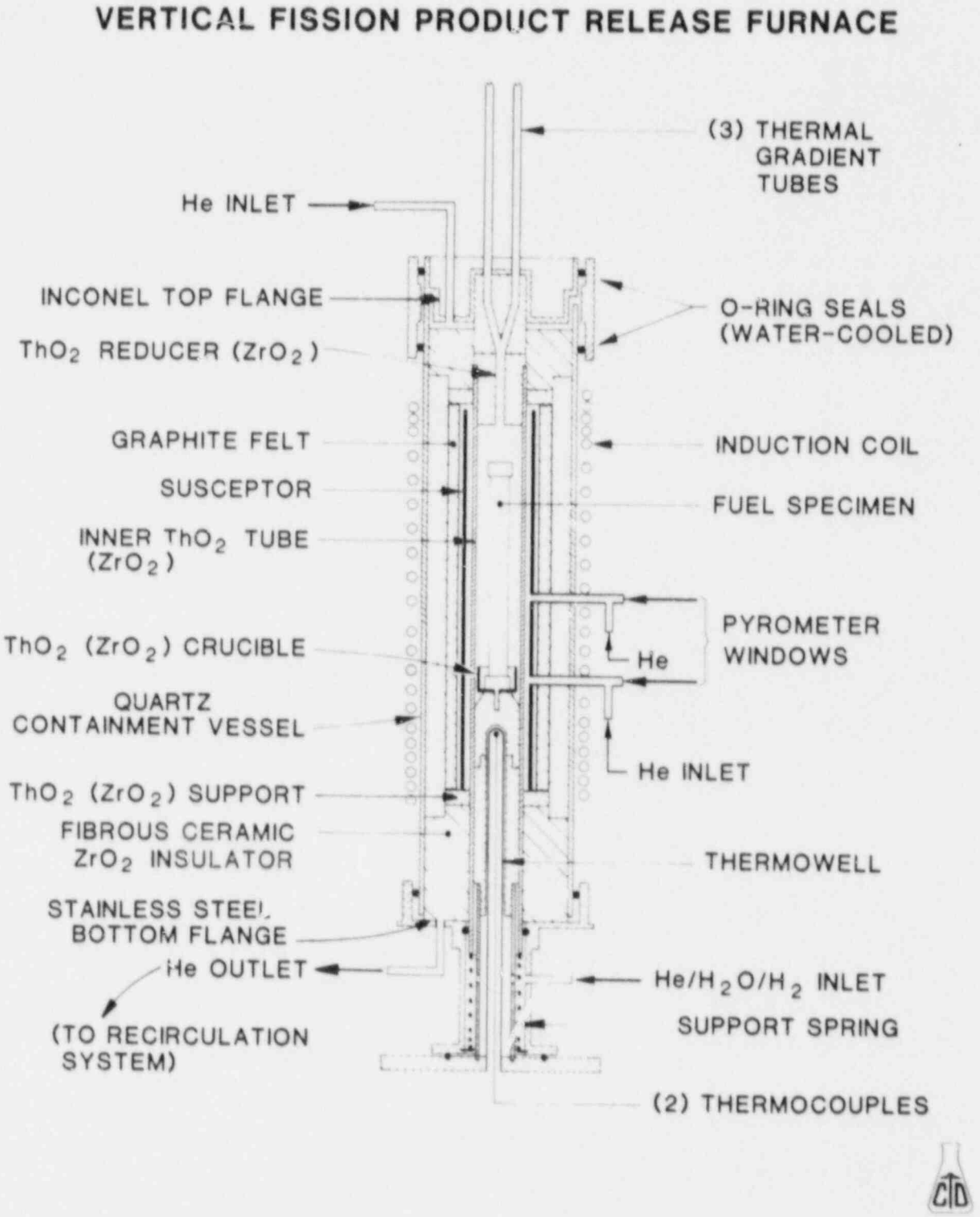

Fig. 2. Vertical fission product release furnace.

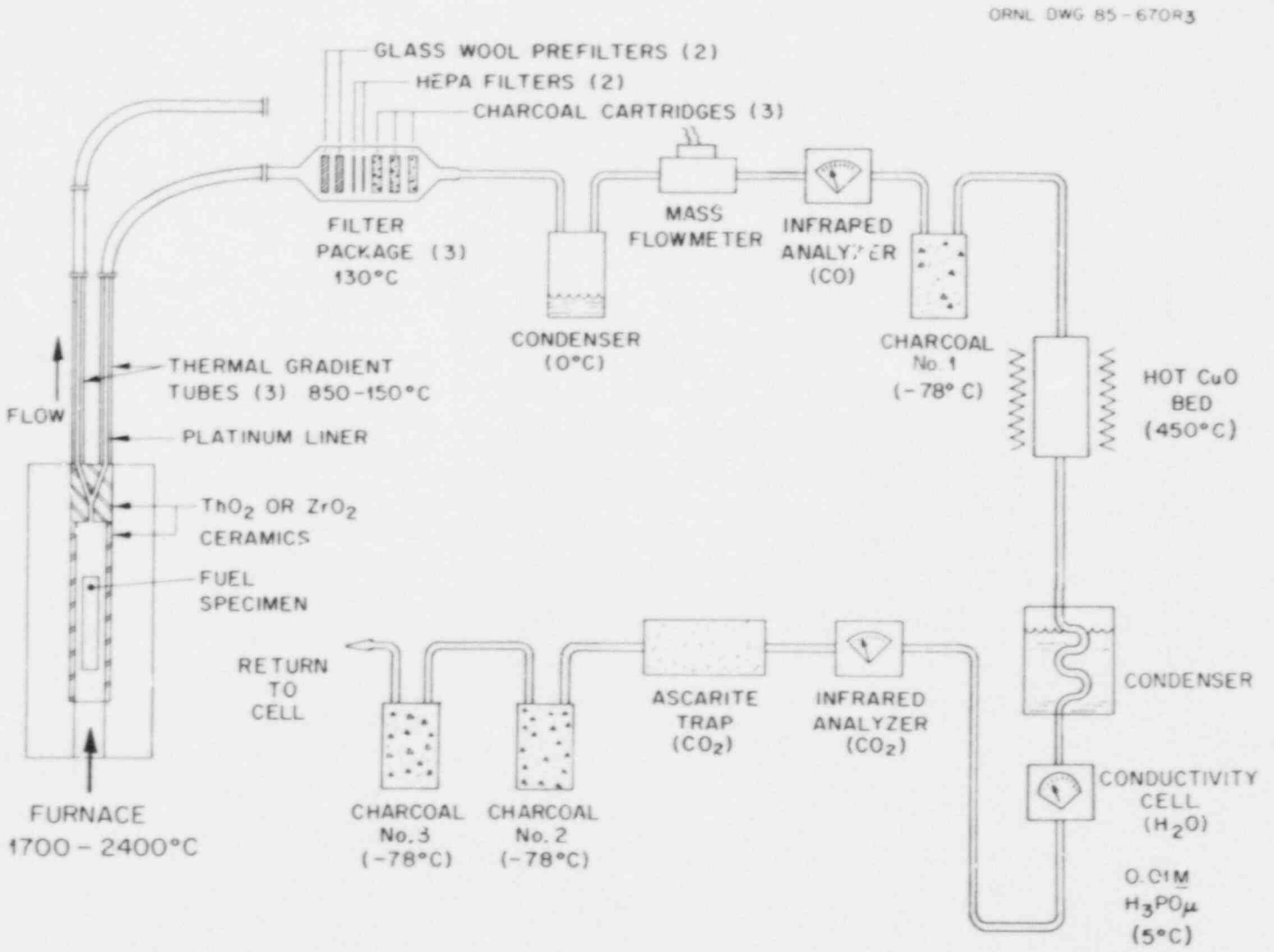

Fig. 3. Fission product collection trains and an effluent analyzing system.

$$Zr + 2H_2O = ZrO_2 + 2H_2 \quad (3)$$

and

$$C + H_2O = CO + H_2 \ . \quad (4)$$

The effluent gas, less the steam, subsequently passed through a stainless steel tube containing copper oxide heated at 720 K, which converted the hydrogen and CO to H_2O and CO_2 as indicated by the following reactions:

$$CuO + H_2 = Cu + H_2O \quad (5)$$

and

$$CuO + CO = Cu + CO_2 \ . \quad (6)$$

Further downstream, the converted effluent gas was passed through a condenser to condense the steam from the reaction shown in Eq. (5) which was collected in a calibrated conductance cell cooled at 278 K. By measuring the change in conductivity of a known volume of 0.01 M H_3PO_4 caused by the incoming condensate, the hydrogen produced from the reactions shown in Eqs. (3) and (4) could be measured with time. The total hydrogen was checked at the end of the test by measuring the decreased weight of the CuO cell. The CO_2 was continuously monitored by a calibrated infrared analyzer and then collected by an Ascarite trap and weighed. As can be seen in Eq. (4), the measurement of CO as CO_2 was also a measurement of the hydrogen produced by the steam/graphite reaction. By subtracting this amount of hydrogen from the total hydrogen (as measured with the conductivity cell), the quantity of hydrogen produced from the steam/Zircaloy reaction could be determined with time.

A data acquisition system (Fig. 4) was used to record the data at 1-min intervals. Several individual chart recorders were used to continuously record temperatures and flow rates. A detailed description of the vertical furnace apparatus has been given elsewhere.[12]

3.2 SPECIMEN

The test specimen was either a 15.2-cm-long Zircaloy tube containing unirradiated UO_2 pellets or a 15.2-cm-long section of an irradiated fuel rod from Oconee Unit One reactor. Zircaloy end caps were placed on the ends of the specimens. Schematics and the characteristics of these specimens are shown in Fig. 5 and in Table 1, respectively.

3.3 TEST CONDITIONS

Specimen temperatures, heatup rates, and nominal gas flow rates for the three cladding oxidation tests are summarized in Table 2, and temperature histories are shown in Fig. 6.

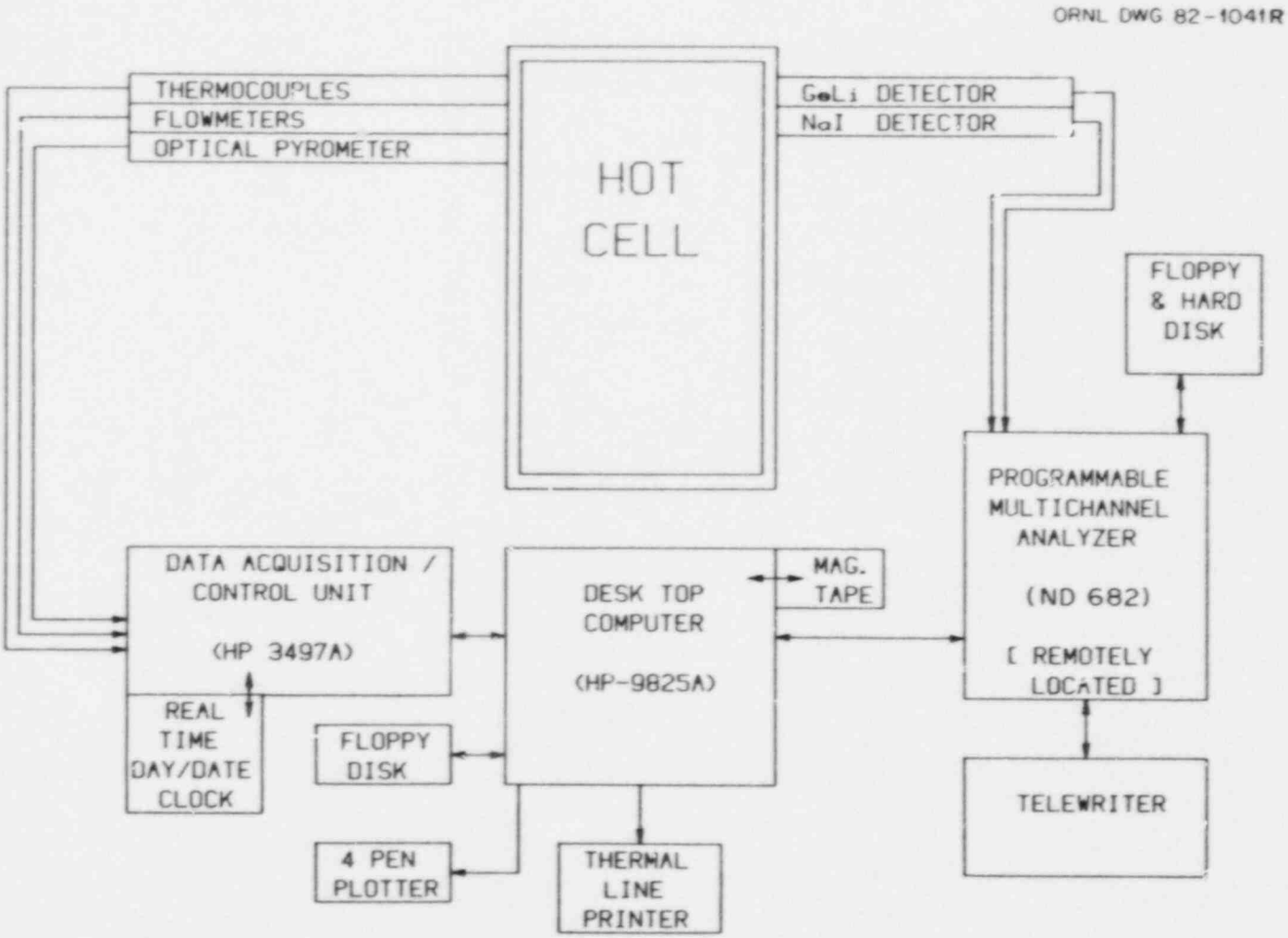

Fig. 4. Data acquisition and processing system for the fission product release tests.

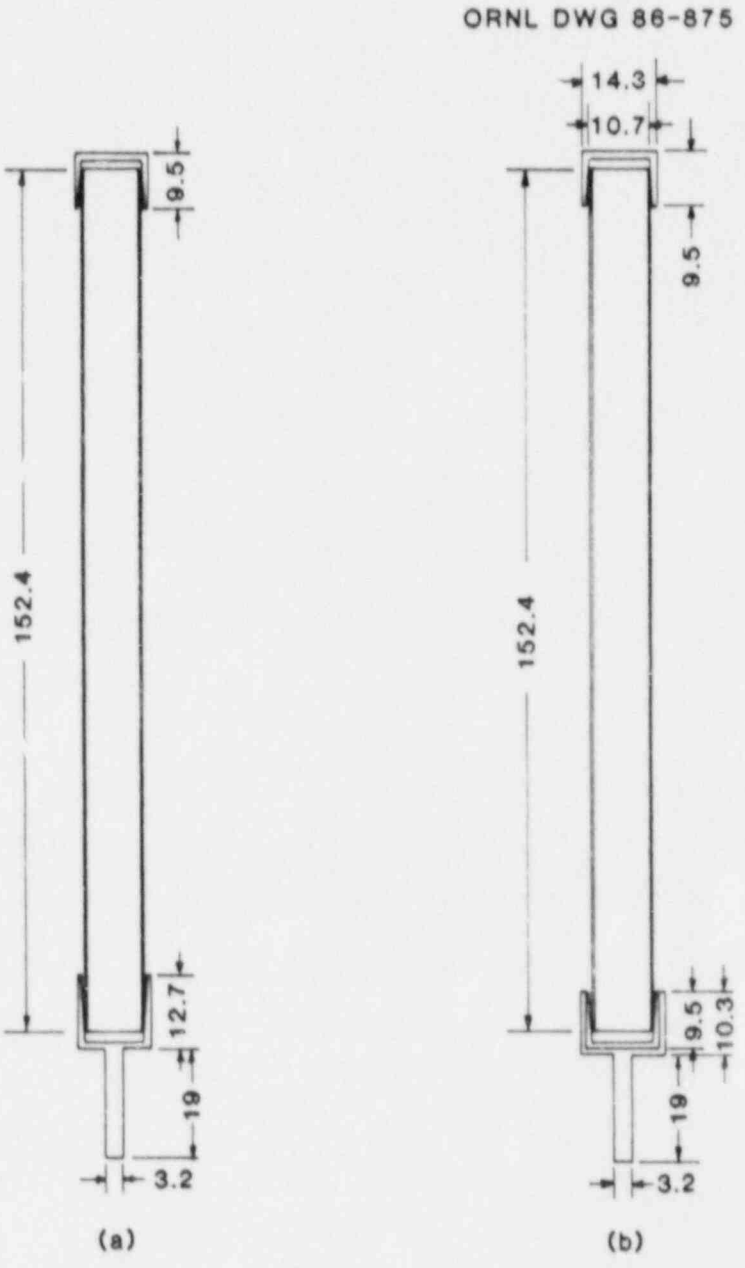

Fig. 5. Zircaloy cladding specimens. (a) Tests VT-3 and VT-12; (b) test VI-1.

Table 1. Test specimen characteristics

	VT-3	VT-12	VI-1
Cladding tube			
Length, mm	152.4	152.4	152.4
OD, mm	10.92	10.92	10.72
ID, mm	9.58	9.58	9.48
Weight, g	21.64	21.67	19.45
End cap (top)			
Length, mm	9.53	9.53	9.53
OD, mm	12.58	12.58	12.70
ID, mm	10.92	10.92	10.72
Weight, g	2.42	2.43	3.02
End cap (bottom)			outer cap
Length, mm	12.65	12.65	10.32
OD, mm	12.58	12.58	14.29
ID, mm	10.92	10.92	12.70
Weight, g	3.95	3.95	5.69
			inner cap
Length, mm	-	-	9.53
OD, mm	-	-	12.70
ID, mm	-	-	10.72
Weight, g	-	-	3.02

Table 2. Summary of operating data

	VT-3	VT-12	VI-1
Specimen temperature, K			
At start of heatup ramp	500	500	500
During first 20-min period	1480[a]	1390	1410
During second 20-min period	1973[b]	2000	2020
During third 20-min period	-	2280	2300
Heatup rate (K/s)	1.0	0.8	1.0
Nominal gas flow rate, L/min			
He into furnace	0.50	0.78	0.80
Steam into furnace	1.2	2.0	1.8
Total H_2 generated, mol	0.496	2.098	1.961
Total CO generated, mol	0.147	1.492	NA[c]
Weight loss of CuO, g	10.41	NA	NA
Weight gain of fuel specimen, g	4.904	NA	NA

[a]Heating period was 4 min.
[b]Heating period was 3 min.
[c]NA = not analyzed.

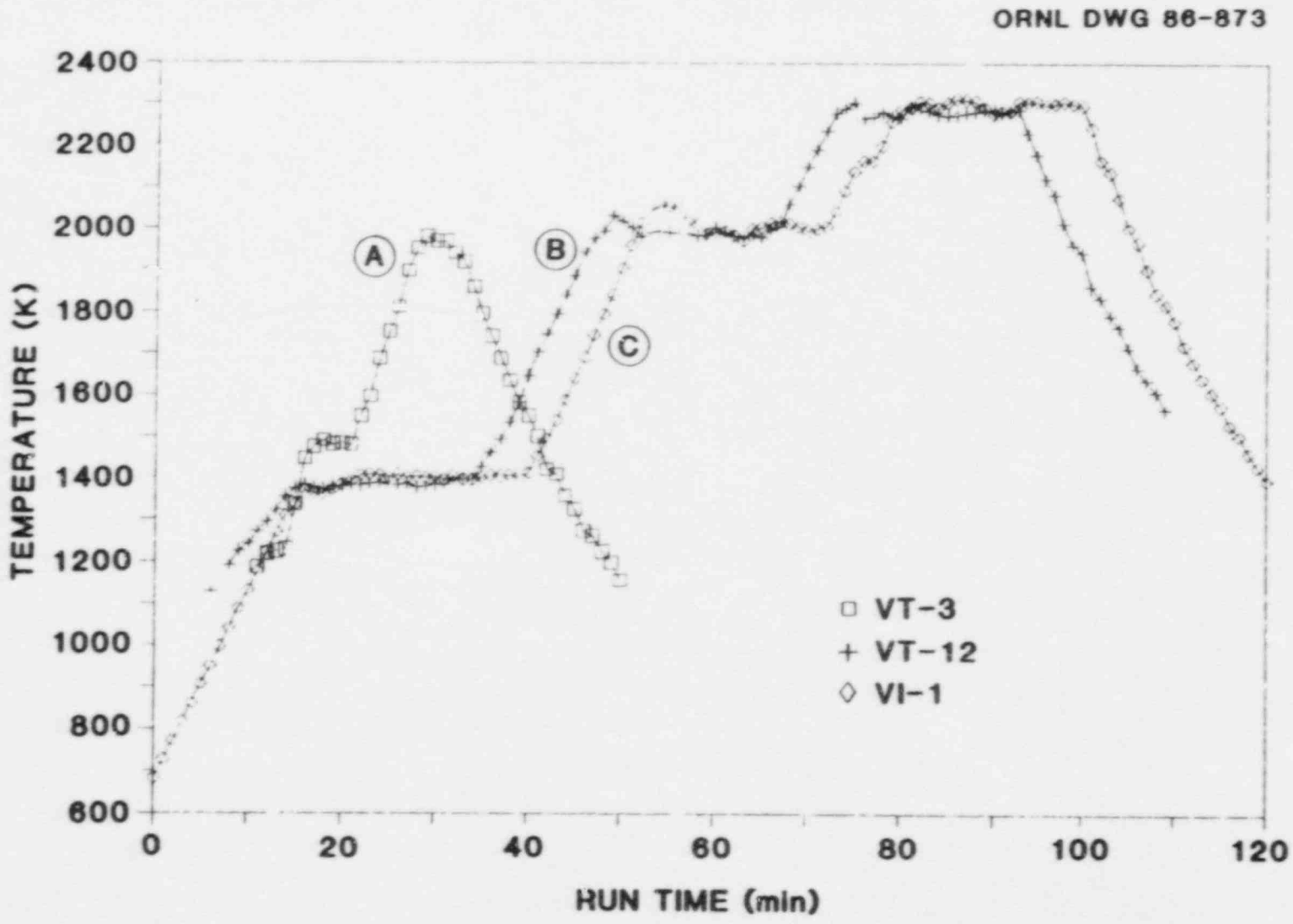

Fig. 6. Temperature histories of cladding oxidation for tests VT-3, VT-12, and VI-1.

4. EXPERIMENTAL RESULTS

4.1 TEST VT-3

Test VT-3 was intended to examine how uniformly the Zircaloy cladding was oxidized under a steam-starved condition. A fuel specimen with a fresh-surface Zircaloy sheath, as illustrated in Fig. 5(a), was heated in flowing steam (1.2 L/min at 298 K) at a rate of ~1 K/s. After the specimen was oxidized at temperatures of 1480 K for 4 min and at 1973 K for 3 min, it was cooled to room temperature at a rate of ~0.8 K/min. The temperature history is shown as curve A in Fig. 6.

Figure 7 is a photograph of the oxidized cladding after the test. The bottom half of the tube was heavily oxidized but the upper half was not. Samples of cladding were analyzed by neutron activation to determine the degree of oxidation. The results showed that the top, middle, and bottom were 19, 44, and 75% oxidized, respectively.

The total hydrogen and CO generated in the furnace was measured by the weight loss of the CuO bed and the weight gain of the fuel cladding during the test and is summarized in Table 2. The oxidation of the cladding was calculated in three different ways: (1) from the values of total hydrogen and CO generated, (2) from the values of weight loss of CuO and total production of CO, and (3) from the value of weight gain of the cladding tube itself. The average axial oxidation calculations were 58, 59, and 53%, respectively. The first two values are slightly higher than the last one, which should be a more accurate average oxidation value. The higher average oxidation values can be explained by additional hydrogen production by the reaction of steam with the tantalum sheath of the thermocouple that helped shield the thermocouple from the induction field.

4.2 TEST VT-12

Test VT-12 was performed under fully-oxidizing conditions. The amounts of hydrogen and CO formed in the furnace were measured continuously in addition to measuring the total hydrogen and CO. A new fuel specimen, similar to that used in test VT-3, was heated at a rate of ~0.8 K/s with a steam supply rate of 2 L/min at 298 K. The temperature history is shown by curve B in Fig. 6; the specimen was kept at 1390, 2000, and 2280 K for 20 min at each temperature. Although the maximum test temperature of 2280 K greatly exceeds the melting temperature of Zircaloy, 2098 K,[13] clad melting did not occur because the cladding should have been completely oxidized during the two lower temperature heating periods.

Measured accumulation and production rates of hydrogen from the Zircaloy/steam reaction are plotted as a function of run time in Fig. 8, together with the total hydrogen accumulation and temperature variation. The hydrogen production rate shown in the figure is multiplied by the factor 20 for easy comparison with the other curves. The production of

ORNL PHOTO 5763-85

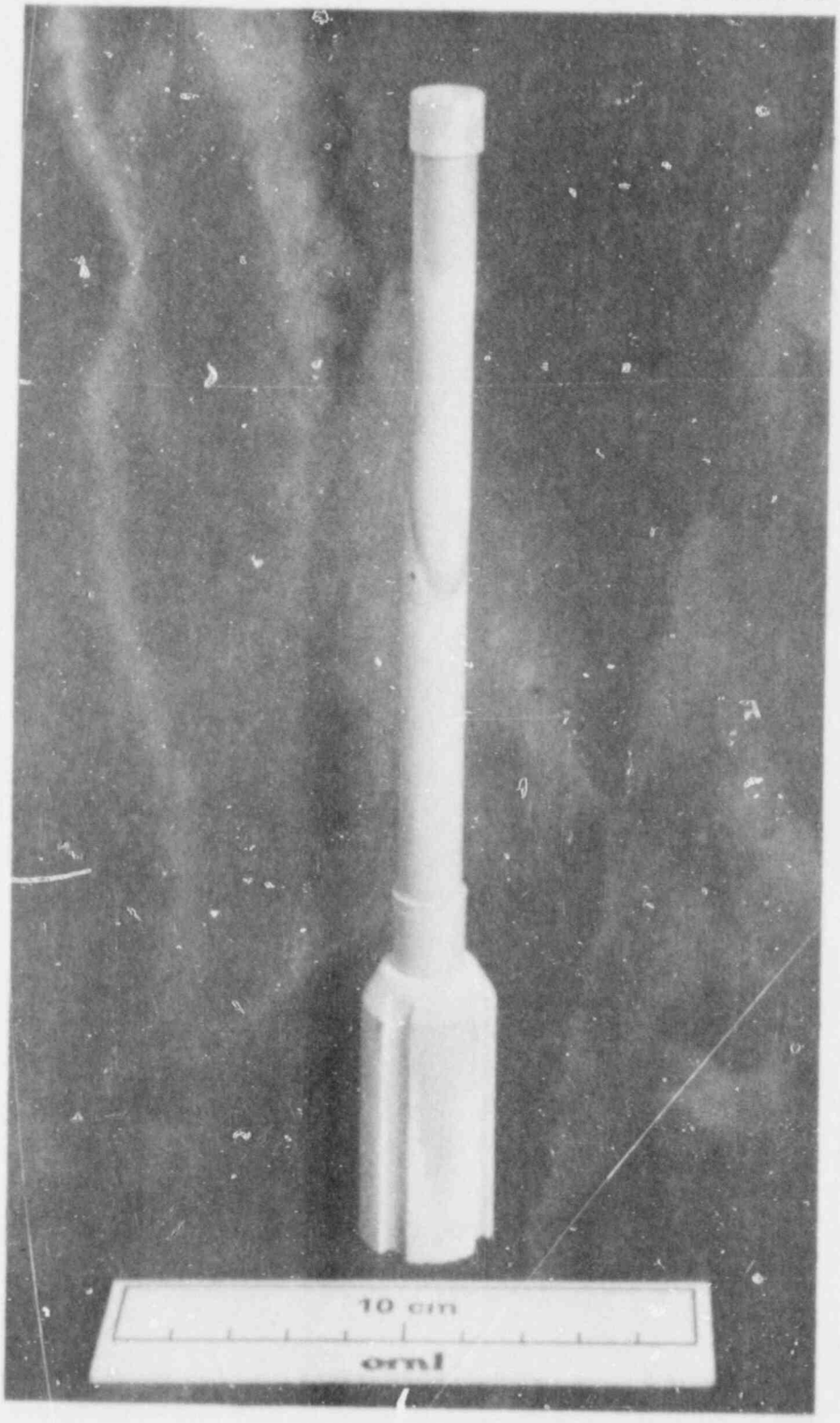

Fig. 7. Appearance of the test VT-3 specimen after oxidation.

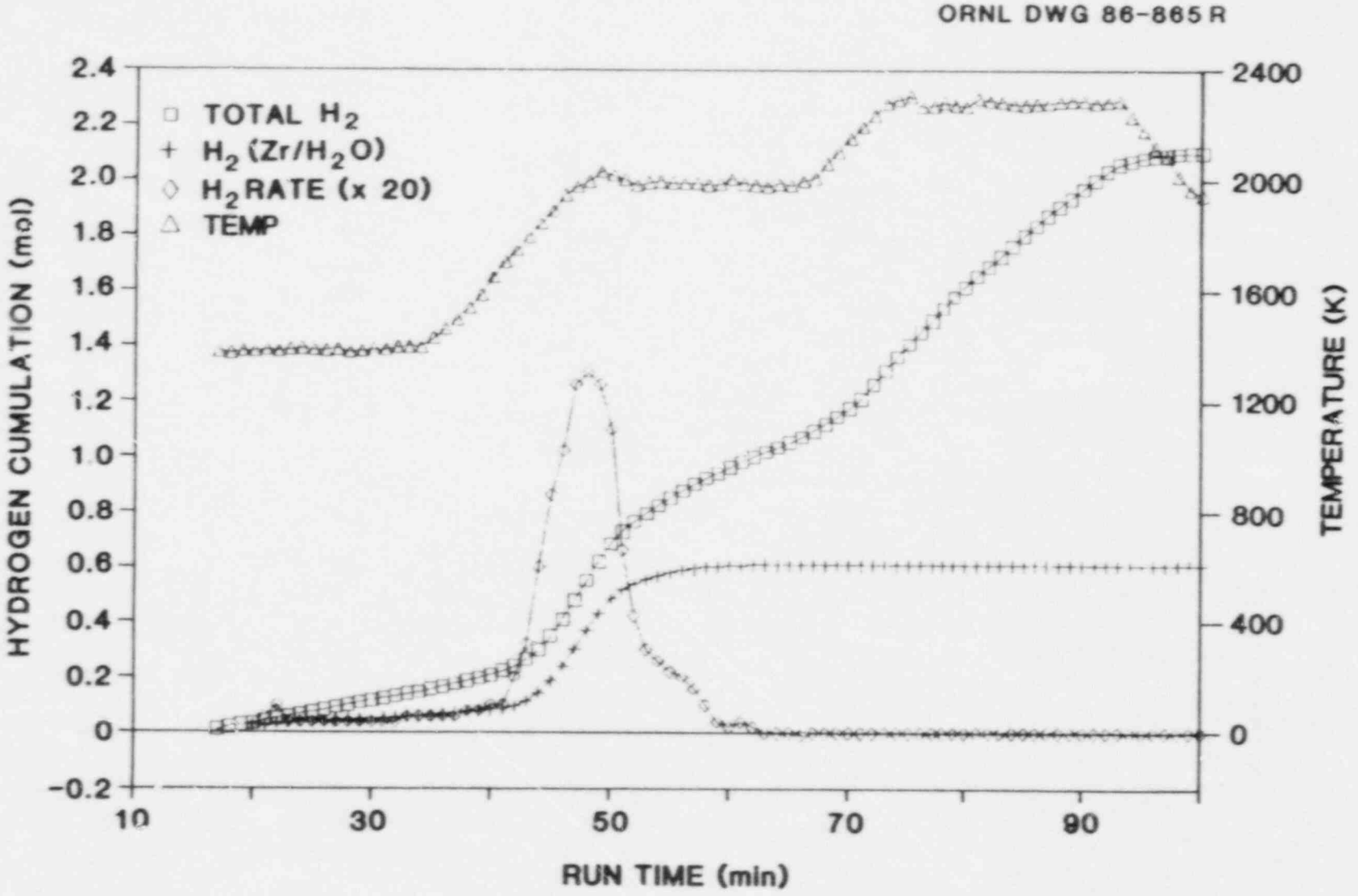

Fig. 8. Hydrogen production measured in test VT-12.

hydrogen by the Zircaloy/steam reaction ceased after 63 min of run time, which was in the second 20-min heating period. A small tailing in the hydrogen production rate curve is attributed to the extra time needed to oxidize the thicker walls of the Zircaloy end caps [see Fig. 5(a)]. A considerable amount of hydrogen was also produced by the graphite/steam reaction, especially during the highest temperature period.

4.3 TEST VI-1

Oxidation behavior of the real fuel specimen, which was cut from a commercially-irradiated fuel rod from the Oconee Unit One reactor, was examined under conditons essentially identical to those of test VT-12. The cladding was slightly oxidized during irradiation in the reactor and the difference in the cladding oxidation behavior caused by the slight initial oxidation was of interest. The heating conditions and temperature history are shown in the fourth column of Table 2 and as curve C in Fig. 6, respectively. The heatup and cooldown rates were ~1 K/s. Unlike in tests VT-3 and VT-12, cold charcoal traps were used in test VI-1 to collect the krypton and xenon fission gas. Unfortunately, there was also a partial holdup of the CO in these traps, which prevented useful information about CO being obtained. This difficulty has since been circumvented by adding a continuous CO monitor before the cold trap and measuring the CO after passing through a single cold trap.

The hydrogen production rate and its accumulation are plotted against run time in Fig. 9. The temperature variation is also included in the figure for better understanding. There are two peaks in the hydrogen production rate curve — a sharp, short-period peak and a smaller and longer-lasting peak. By comparing the total hydrogen accumulation curve with that of test VT-12, it can be seen that the first peak is mainly attributed to the Zircaloy/steam reaction, and that the second one is presumably caused by the graphite/steam reaction. There is a flat region between the peaks where the hydrogen production rate is constant. As seen in the figure, the fuel temperature during this time period was kept constant at 2000 K. Since the reaction rate of the graphite/steam reaction is assumed to be constant at a single temperature, the hydrogen accumulation in this period must have been produced mainly by the graphite/steam reaction. If the hydrogen was produced by the Zircaloy/steam reaction, the hydrogen production rate should have decreased with heating time because the isothermal Zircaloy cladding oxidation is governed by the parabolic reaction rate law.[14-16] The increased hydrogen production at 77 min is presumed to be the result of a sudden increase in the rate of leakage of steam into the graphite susceptor region. Steam leakage into the susceptor region during test VT-12 was apparently much less than during test VI-1.

5. THE OXIDATION MODEL

A simple method was developed to calculate the extent of Zircaloy cladding oxidation and resultant hydrogen production in the vertical furnace tests. The main concerns of the model are how much Zircaloy has

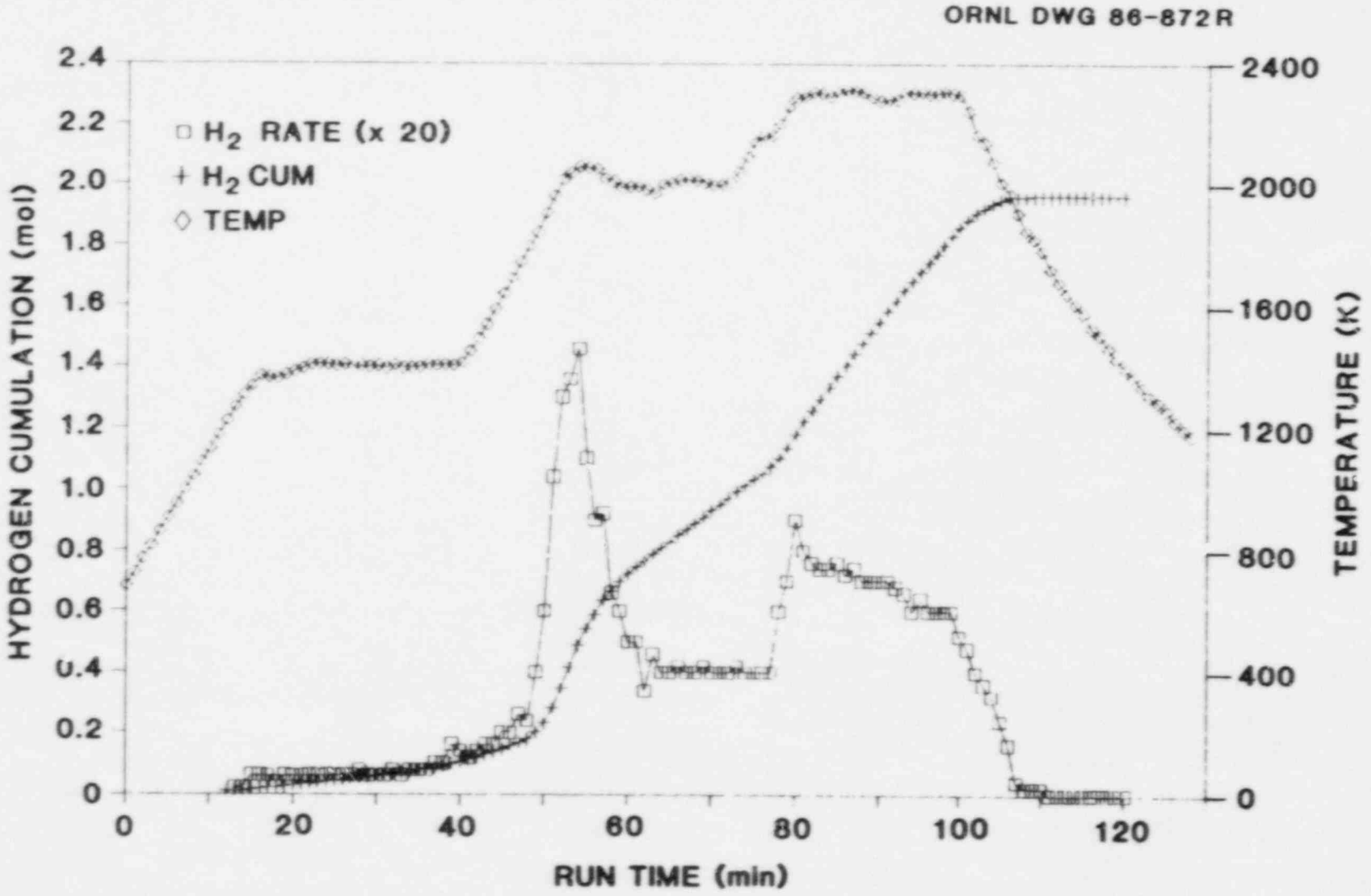

Fig. 9. Hydrogen production measured in test VI-1.

reacted with steam and how much hydrogen has been generated. The product of the Zircaloy/steam reaction is treated as ZrO_2. Evaluation of the detailed phase structure in the reaction product[17] and of the interaction between the cladding and UO_2 fuel[18] are beyond the scope of the model.

5.1 OXIDATION KINETICS

It is widely accepted that the oxidation kinetics of zirconium alloys such as Zircaloy-2 and -4 is described by the parabolic rate law at temperatures above 1273 K in air or in steam atmospheres.[14-16,19,20] In this model, the oxidation kinetics of Zircaloy in steam is assumed to be described by the parabolic rate law over the whole temperature range until the cladding is completely oxidized. It should be recognized, however, that parabolic rates for any of the kinetic parameters describing the oxidation of Zircaloy are strictly applicable only for "semiinfinite" specimen geometry. To apply a parabolic rate for the consumption of metal derived from this condition to the extended or complete oxidation of a thin-walled tube is only an approximation. However, it turns out that this model of the reaction kinetics is in good agreement with the experimental data.

For isothermal oxidation, the parabolic equation is:

$$W^2 = kt \tag{7}$$

where

W = the amount of zirconium per unit surface area oxidized (kg/m^2),
k = the parabolic rate constant, $(kg/m^2)^2/s$,
t = a reaction time, s.

The parabolic rate constant has the form

$$k = k_0 \exp(-Q/RT) \tag{8}$$

where both k_0 and Q are constants, $(kg/m^2)^2/s$ and J/mol, respectively, R is the gas constant, 8.31 J/(mol K), and T is the absolute temperature, K. Selected values for the constants k_0 and Q are listed in Table 3 and the temperature dependence of k is shown in the Arrhenius plot in Fig. 10. Data obtained by Pawel et al.[16] and by Prater and Courtright[21] have been combined to cover the whole temperature range in some of our calculations.

The amount of zirconium reacted cannot be calculated directly with Eq. (7) if the parabolic rate constant changes during the oxidation cycle as the result of a temperature change. The ZIRCOX model uses a stepwise calculation that is easy to use in a spreadsheet program on a personal computer. We usually calculate oxidation at 1 min intervals for our test conditions. More frequent timesteps can be used for greater accuracy if desired.

Table 3. Selected values k0 and Q for the parabolic rate constant $k = k_0 \exp(-Q/RT)$ for Zircaloy oxidation in steam

Investigators	Temperature range (K)	k_0 (kg^2/m^4s)	Q (kJ/mol)	Reference
Baker and Just	1273 ~ mp	3.33E+03	190	14
Urbanic and Heidrick	1323 ~ 1853	2.96E+01	140	15
	1853 ~ mp	8.79E+01	138	
Pawel et al.	1273 ~ 1773	2.94E+02	167	16
Prater and Courtright	1783 ~ 2773	2.68E+04	220	21

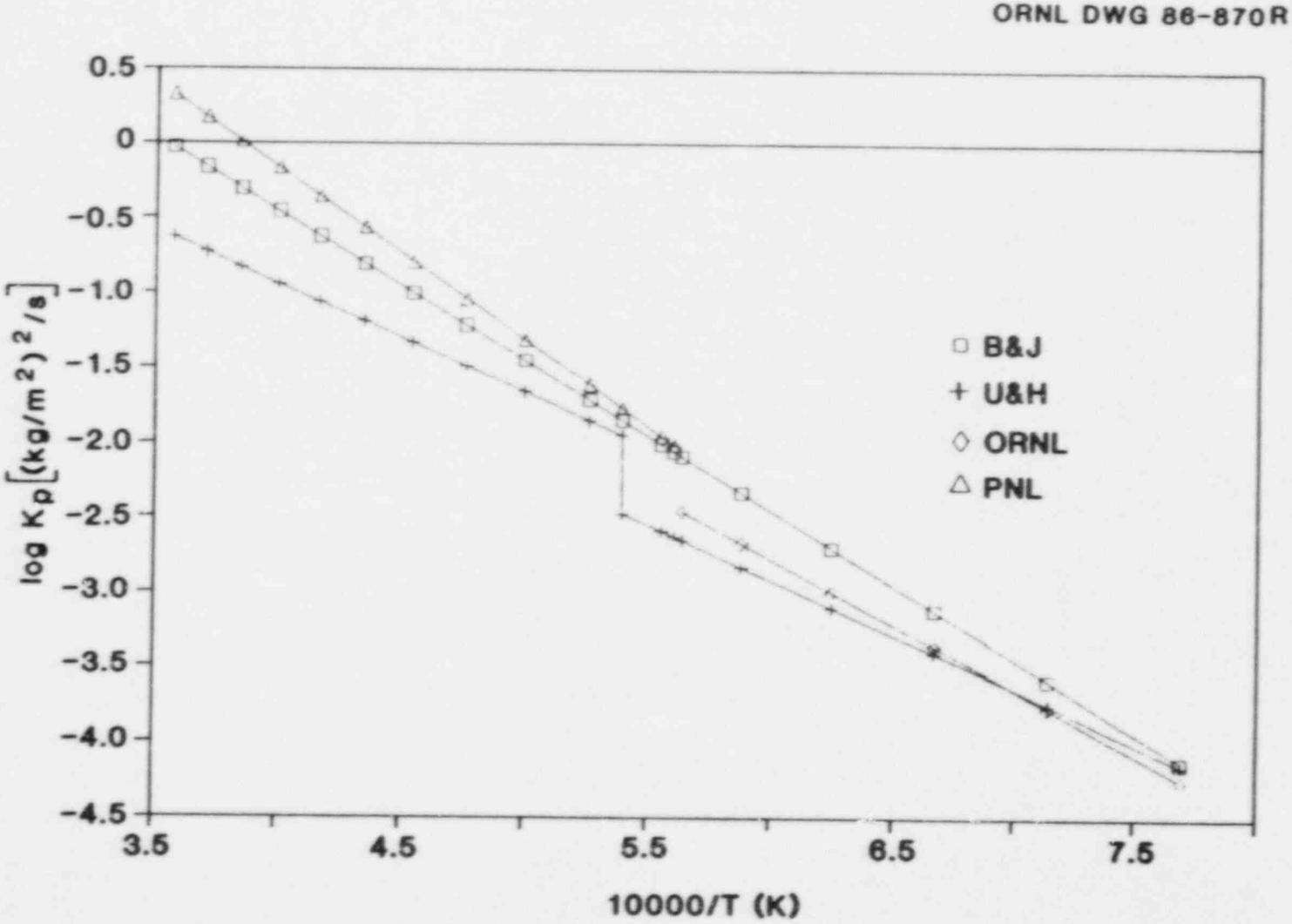

Fig. 10. Comparison of parabolic rate constants for Zircaloy oxidation. B&J: Baker and Just; U&H: Urbanic and Heidrick; ORNL: Pawel et al.; and PNL: Prater and Courtright.

At each new timestep (timestep n), ZIRCOX calculates four different quantities in this order: (1) k_n using Eq. (8), (2) t^* using Eq. (9), (3) W_n^2 using Eq. (10), and (4) the amount of steam consumed. The equations for calculating t^* and W_n^2 are:

$$t_n^* = W_{n-1}^2/k_n \ , \tag{9}$$

$$W_n^2 = k_n(t_n + t_n^*) \tag{10}$$

where

t_n^* = time at new k_n required to form W_{n-1}, s,
t_n = time of the new timestep, s,
W_{n-1} = total mass of zirconium per unit area calculated to have reacted at end of previous timestep, kg/m^2,
k_n = the parabolic rate constant at new timestep temperature, $(kg/m^2)/s$,
W_n = total mass of zirconium per unit area calculated to have reacted by the end of the new timestep, kg/m^2.

This calculational procedure is unusual in that ZIRCOX does not calculate directly the amount of zirconium oxidized in each time step. ZIRCOX calculates the total amount of zirconium oxidized by making use of t_n^*. This technique derives from the assumption that (W^2) in Eq. (7) can be created by any combination of the product kt in Eq. (7). For each timestep, we assume that (W_{n-1}^2) was formed at the new T_n, k_n, and t_n^*.

This technique is mathematically the same as obtained by summing the individual products $k_n t_n$ as follows:

$$W_n^2 = \sum_{i=1}^{n} k_i t_i \tag{11}$$

or

$$W_n^2 = W_{n-1}^2 + k_n t_n \tag{12}$$

5.2 MODELING OF THE CLADDING SPECIMEN

A drawing of a typical PWR fuel specimen used in the cladding oxidation tests is shown in Fig. 11(a). The fuel specimen has two tapered end caps of Zircaloy. For simplicity of calculations, it is assumed that these end caps have a uniform wall thickness and that there is no overlap between the cladding tube and end caps, as shown in Fig. 11(b). Each cladding specimen has 13 nodes – 2 for end caps and 11 for the cladding tube. The reaction rate is calculated for each node.

5.3 STEAM BALANCE

A steam balance must be made at each node to determine if there is sufficient steam for the oxidation reaction. We assume that the velocity and concentration of steam have no effect on the reaction rate until the steam is completely consumed. The amount of steam flow out from the i^{th} node during the n^{th} time period ($Q_{out,i,n}$) is the difference between the amount of steam flow into the area and that of steam consumption on the node.

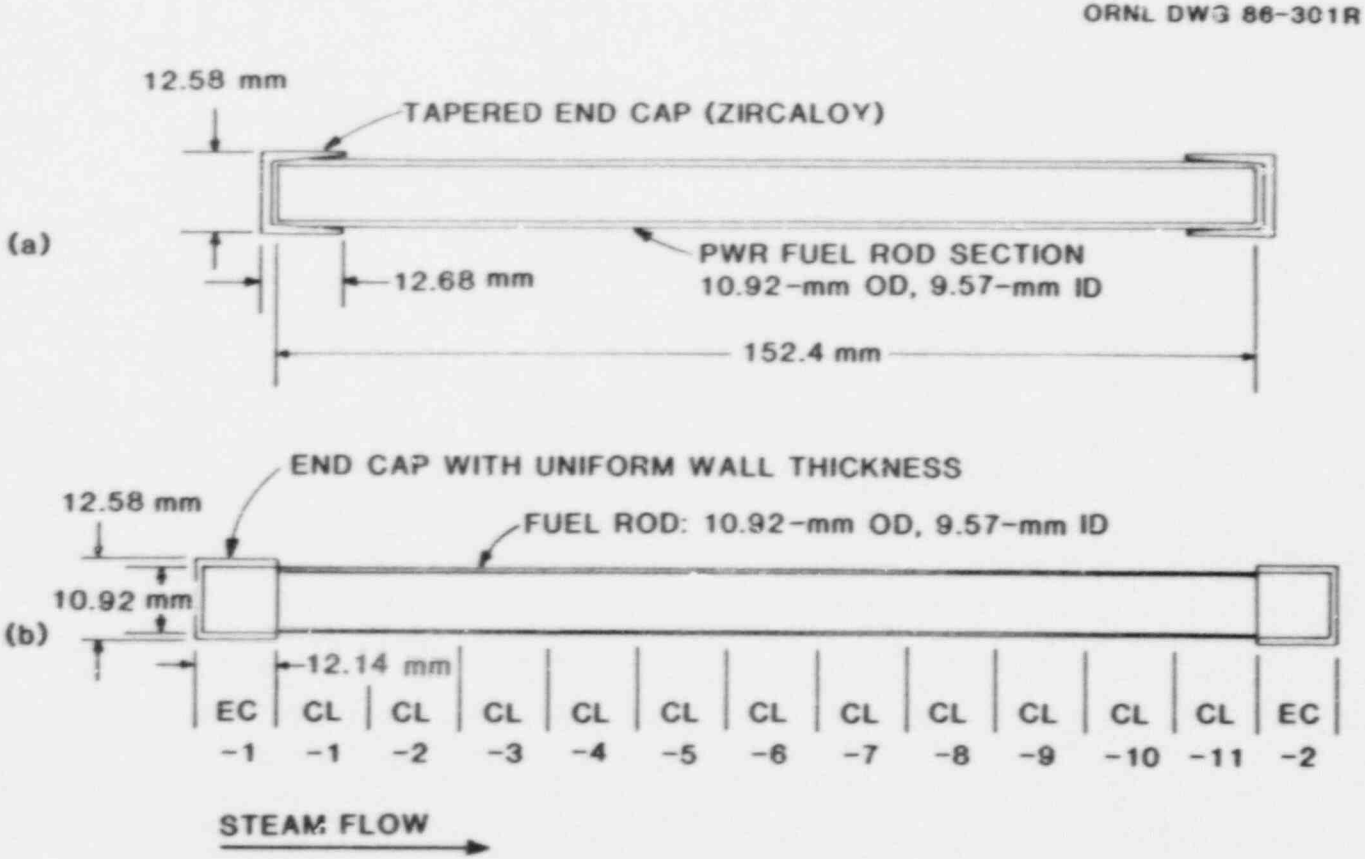

Fig. 11. Model of fuel cladding. (a) Cladding specimen; (b) model of the cladding.

$$Q_{out,i,n} = Q_{in,i,n} - 2\Delta W_{i,n} S_i M_{H_2O}/M_{Zr} \ , \tag{13}$$

$$\Delta W_{i,n} = W_{i,n} - W_{i,n-1} \ , \tag{14}$$

$$W_{i,n} = k_{i,n}(t_n^* + t_n)^{1/2} \ , \tag{15}$$

where

$(W_{i,n})$ = total amount of Zr reacted per unit surface at end of the n^{th} period, kg/m^2,
Q = amount of steam, kg,
t_n = time of the n^{th} period, s,
S_i = surface area of the ith node, m^2,
M_{Zr} = atomic weight of zirconium, 0.091 kg,
t^* = effective time from Eq. (9), s.

At each node, the weight gain must not exceed the steam supply. The surface area of the i^{th} node, S_i, is given by:

$$S_i = m_i \ C/d \ l_i \ , \tag{16}$$

where

m_i = weight of the i^{th} node, kg,
C = correction factor for zirconium content, 0.985,
l_i = wall thickness of the i^{th} node, m,
d = density of zirconium, 6.50×10^3 kg/m^3.

5.4 CALCULATION OF THE CLADDING OXIDATION

Cladding oxidation calculations were performed for tests VT-3, VT-12, and VI-1 using three sets of Zircaloy oxidation rate constants.[14-16,19] The Urbanic and Heidrick rate constant (U&H) is the lowest at high temperatures (where the Zircaloy/steam reaction becomes significant), and the combined rate constant of Pawel et al. and Prater and Courtright (PPC) is the highest. Oxidation calculations using Baker and Just data (B&J) were also carried out to compare the results with those of the other two. Until recently, the data of Baker and Just have been used as the standard for Zircaloy oxidation in evaluating postulated LWR accidents.

Input data for the Zircaloy oxidation calculations are summarized in Table 4. Since the temperature measurements were carried out at one minute intervals, the time interval of each step is also one minute.

Temperatures were observed by means of optical pyrometers and were corrected to the fuel temperatures through the following empirical equations.[22] The correction to the pyrometer for glass and mirror surfaces is given by:

$$T(true,K) = 1/[1/\{T(meas) + 273.2\} - 0.0000165] \ , \tag{17}$$

Table 4. Input data for Zircaloy oxidation calculation

	VT-3	VT-12	VI-1
Steam supply rate, mol/min	2.25E-02[a]	8.18E-02	7.36E-02
Time interval, min	1	1	1
Weight, kg			
EC-1	3.95E-03	3.95E-03	5.69E-03[b]
			3.02E-03[c]
CL-1 to CL-11	1.97E-03	1.97E-03	1.77E-03
EC-2	2.42E-03	2.43E-03	3.02E-03
Surface area, m^2			
EC-1	7.21E-04	7.21E-04	7.22E-04[b]
			4.61E-04[c]
CL-1 to CL-11	4.43E-04	4.44E-04	4.31E-04
EC-2	4.42E-04	4.43E-04	4.61E-04
Limiting W value, kg/m^2			
EC-1	5.39	5.39	7.74[b]
			6.44[c]
CL-1 to CL-11	4.37	4.37	4.03
EC-2	5.39	5.39	6.44

[a]Best fit value. To be read as 0.0225.
[b]For an outer end cap.
[c]For an inner end cap.

where T(meas) is the observed temperature reading in °C. An additional correction is needed to obtain the fuel temperature, since the spot on the furnace tube liner viewed by the pyrometers is cooler because of radiant heat losses. This correction is:

$$T(\text{fuel,K}) = 1.0191\ T(\text{true,K}) + 42.52\ . \tag{18}$$

The temperature of each step is defined as:

$$T_n = (T_{n-1} + T_n)/2\ , \tag{19}$$

where $T_n = T(\text{fuel,K})_n$.

The degree of oxidation is calculated by:

$$Ox(\%) = 100\ W/W_{lim}\ , \tag{20}$$

where W is the amount of reacted Zircaloy per unit surface area, and W_{lim} is the limiting reaction amount and is calculated by

$$W_{lim} = l_i\ d\ . \tag{21}$$

The hydrogen production rate (HPR)n at the n^{th} period in mol/min is:

$$(HPR)_n = (SSR) - Q_{out,EC-2,n} , \quad (22)$$

where

(SSR) = steam supply rate, mol/min,
$Q_{out,EC-2,n}$ = amount of steam flow-out from the EC-2 (end cap-2) node during the n^{th} period, mol/min.

The computerized model is named ZIRCOX and is run on an IBM-PC. Although the model was developed for the vertical furnace experiments, the orientation of the fuel rod does not affect the calculation. The oxidation of almost any shape of Zircaloy can be calculated with the model.

A special version of the model, ZIRCOX-M, allows changes in Zircaloy surface area and thickness that result from melting. This version has been used successfully with tests that are not described in this report.

6. COMPARISON OF RESULTS

6.1 TEST VT-12

Results of experimental and calculated cladding oxidation in test VT-12 are summarized in Table 5; the axial temperature gradient was not

Table 5. Results of experimental and calculated cladding oxidation for test VT-12

	Experiment	U&H[a]	B&J[b]	PPC[c]
Time of complete oxidation				
End cap, min	63	68	59	55
Cladding, min	NA[d]	60	54	52
H_2 generated, mol	0.606	0.606	0.606	0.606
Peak H_2/H_2O ratio	3.87	1.13	1.50	3.35
and time, min	48	45	4750	4749

[a]Urbanic and Heidrick data.
[b]Baker and Just data.
[c]Combined ORNL and PNL data.
[d]NA = not analyzed.

taken into account in these calculations. Calculated cladding oxidations in test VT-12 are shown in Figs. 12(a), (b), and (c) using the oxidation rate constants of U&H, B&J and PPC, respectively. Since the steam supply

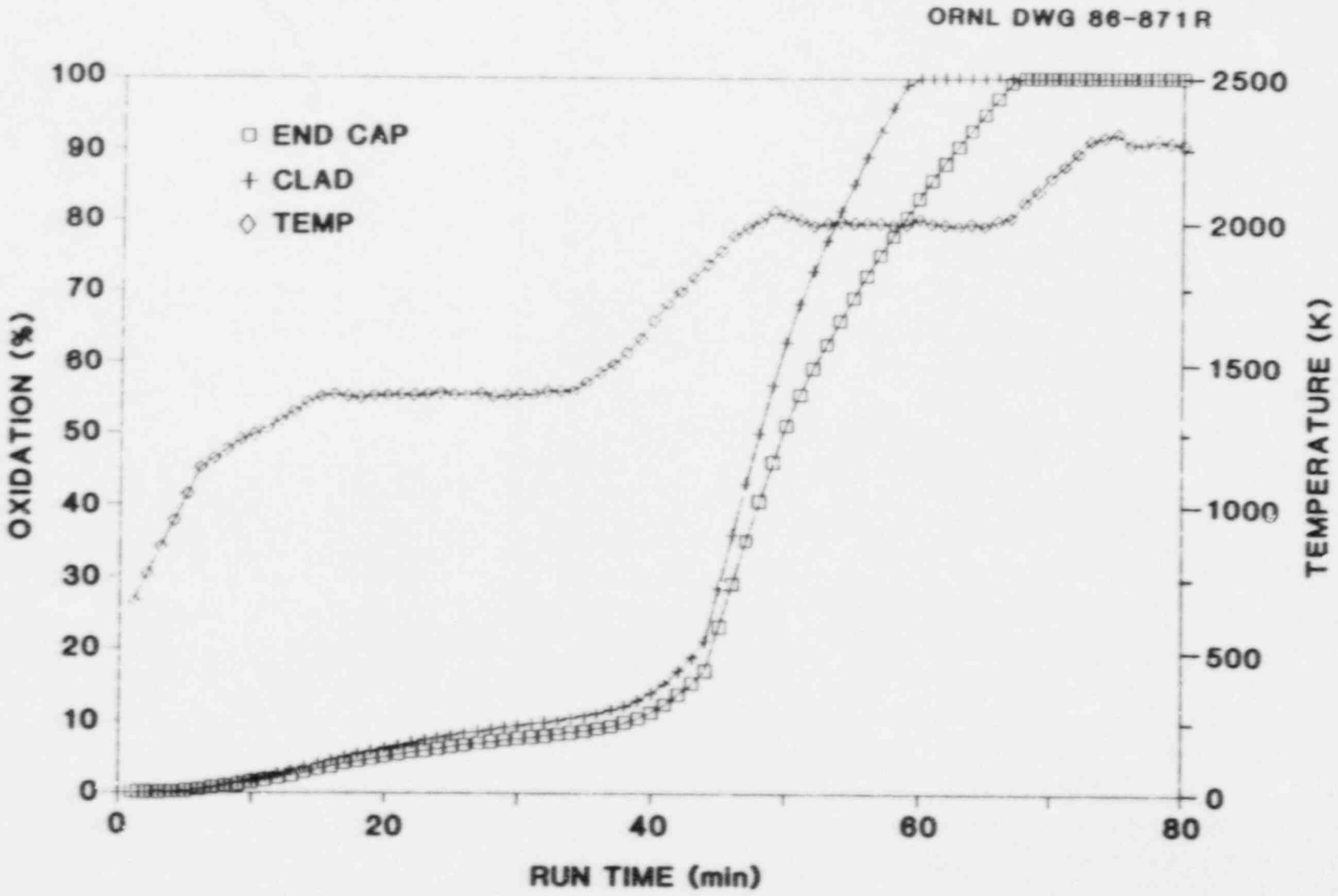

Fig. 12(a). Calculated cladding oxidation using the U&H data for test VT-12.

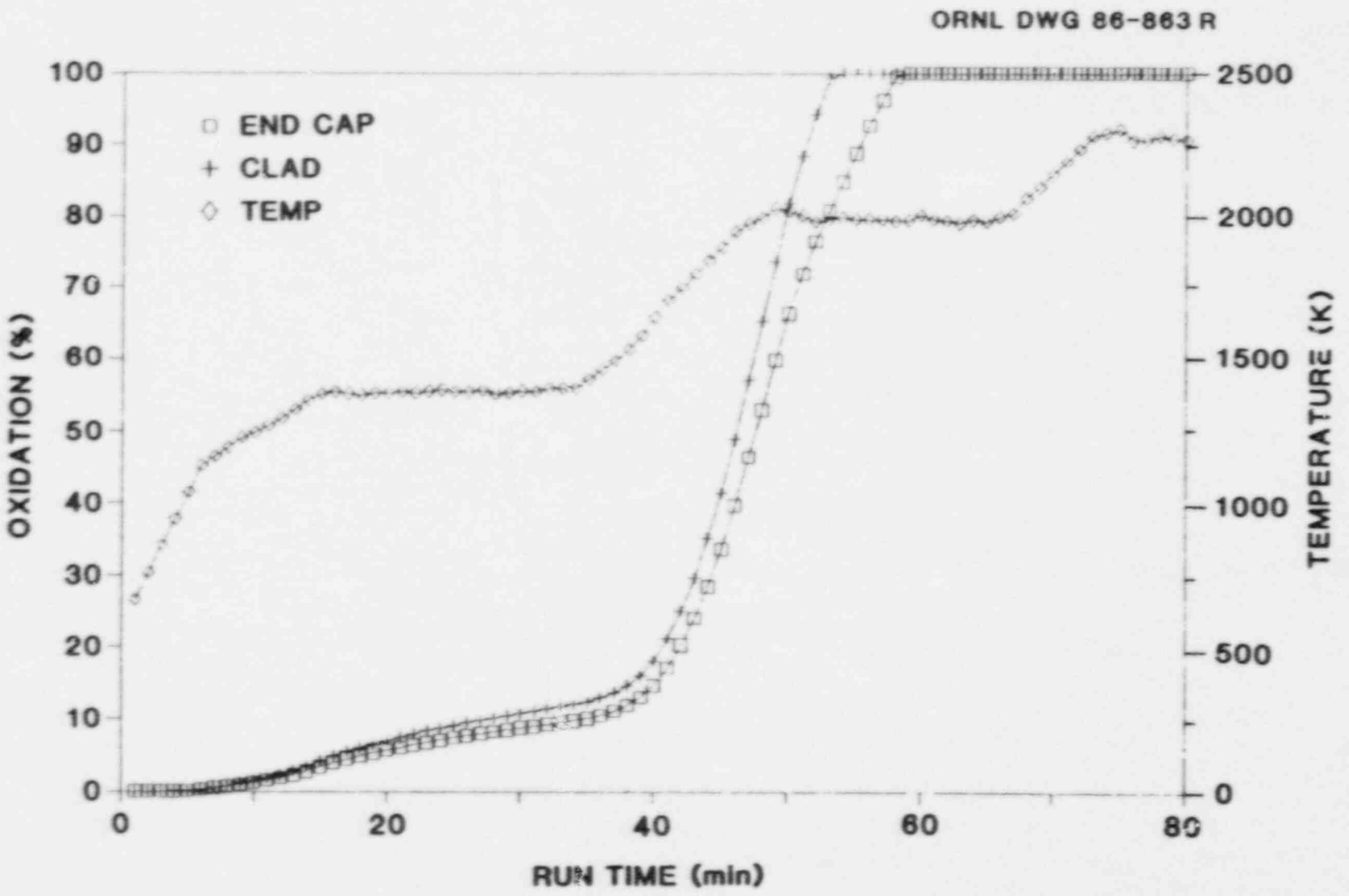

Fig. 12(b). Calculated cladding oxidation using the B&J data for test VT-12.

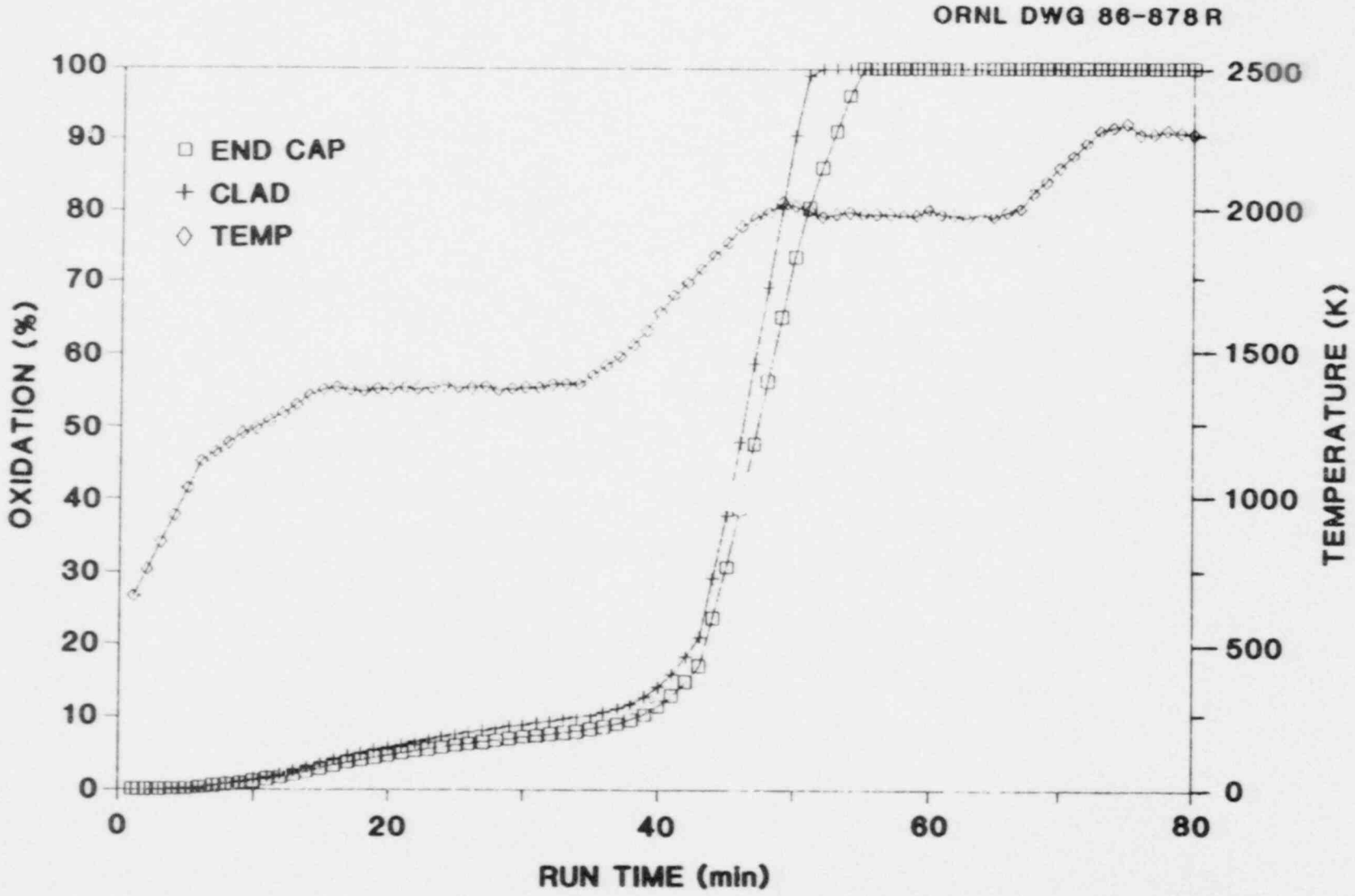

Fig. 12(c). Calculated cladding oxidation using the PPC data for test VT-12.

rate was high enough not to cause steam starvation, the cladding was oxidized uniformly and completely within the second heating period at 2000 K. In these figures, the curves with squares and pluses show the oxidation of end caps and the cladding, respectively; the curve with the diamonds gives the temperature history. In each case the oxidation reaction was faster at temperatures above 1700 K. It took 3 to 8 min longer for the walls of the end caps to be completely oxidized than it did for the wall of the cladding tube because they were thicker.

Calculated hydrogen production rates are plotted in Fig. 13 together with the rates measured experimentally. The experimental values are shown as the curve with squares, the curves with pluses, diamonds and triangles were calculated using the oxidation rate constant of U&H, B&J, PPC, respectively. The PPC curve is in better agreement with the experiment curve. The calculated Zircaloy/steam reaction rate, however, results in an earlier completion of the reaction compared to the experiment. Hydrogen accumulation curves are shown as a function of run time in Fig. 14. Symbols are the same as those defined in Fig. 13. Again, the calculated curve, which was obtained by using the PPC data, agreed well with the curve obtained experimentally. Because of it's low oxidation rate constant at temperatures above 1800 K, the U&H data give a low hydrogen production rate, which results in underprediction in the hydrogen accumulation curve. On the other hand, the high oxidation rate of the B&J data in the temperature range between 1300 and 1800 K causes an overprediction in the hydrogen production.

6.2 TEST VI-1

Calculated and experimental hydrogen production rates for test VI-1 are plotted against run time in Fig. 15. The symbols are the same as those used in Fig. 13. The curve calculated by use of the PPC data agrees best with the first experimental hydrogen production peak, in which hydrogen came mainly from the Zircaloy/steam reaction, as mentioned earlier (see Sect. 4.3). The cladding oxidation during the test, as calculated by using the PPC data, is shown in Fig. 16, together with the temperature history. Since the EC-1 node had two end caps and a combined, much-thicker wall than that of EC-2 [see Fig. 5(b)], it took ~21 min longer for the EC-1 wall to be completely oxidized than for the EC-2 wall. There was a small temperature overshoot after ~54 min of run time as is shown in the figure. This extra heat was probably caused by the heat released from the exothermic Zircaloy/steam reaction. It is estimated that the heat release at the peak region was ~360 W, which was sufficient enough to cause ~50 K temperature difference between the surface of the cladding and the surface of the zirconia furnace tube liner where the temperature was being measured by optical pyrometers.

The difference in temperature between the surface of the cladding and the surface of the zirconia liner was estimated by calculating the fuel and cladding temperatures using the HEATING6 heat transfer computer program[23] with conditions such that the cladding and fuel are hotter than the zirconia liner whenever the Zircaloy/steam reaction is occurring. The zirconia liner and cladding temperatures are shown as a function of

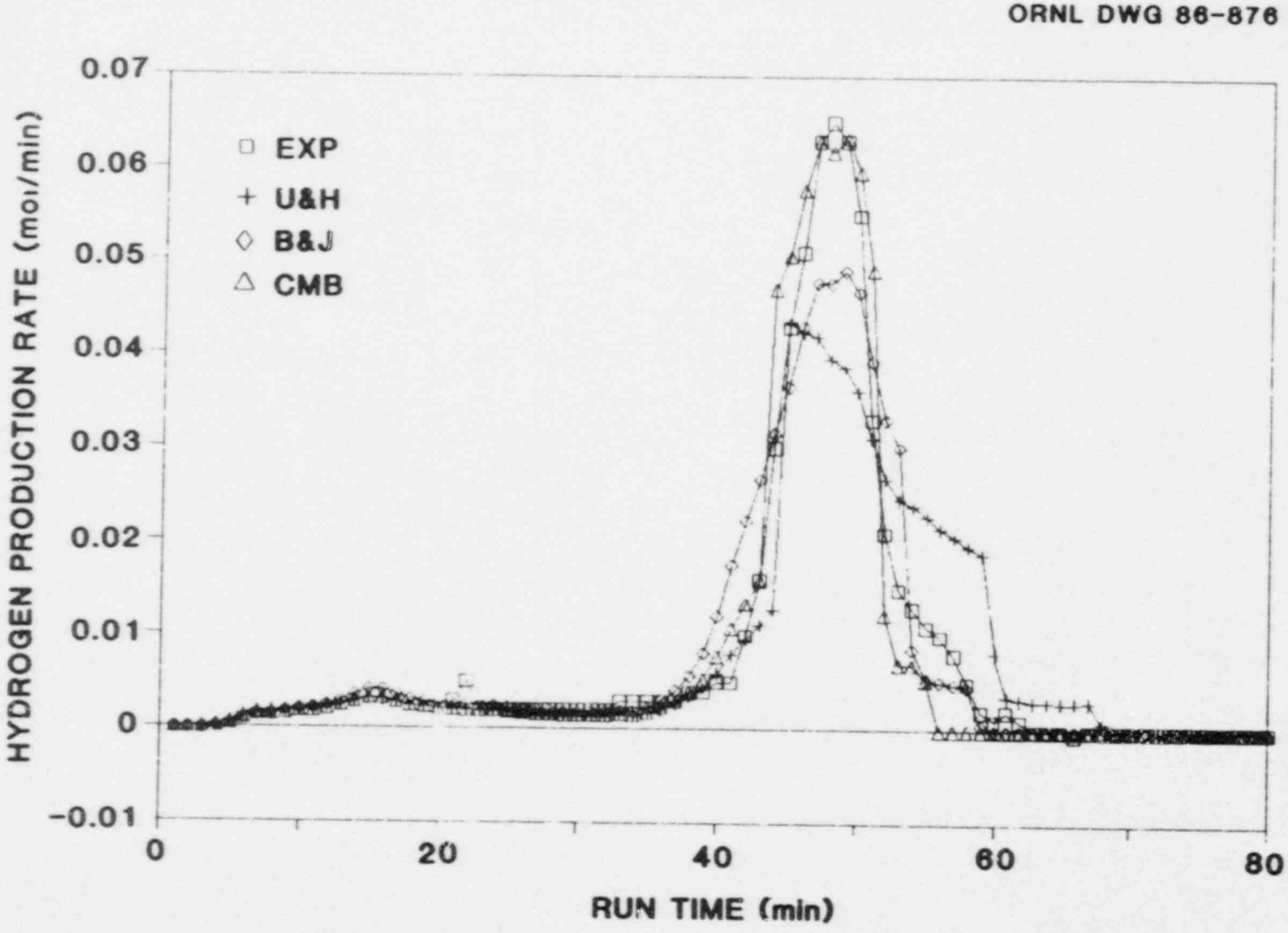

Fig. 13. Comparison of hydrogen production rates from measured and calculated values for test VT-12.

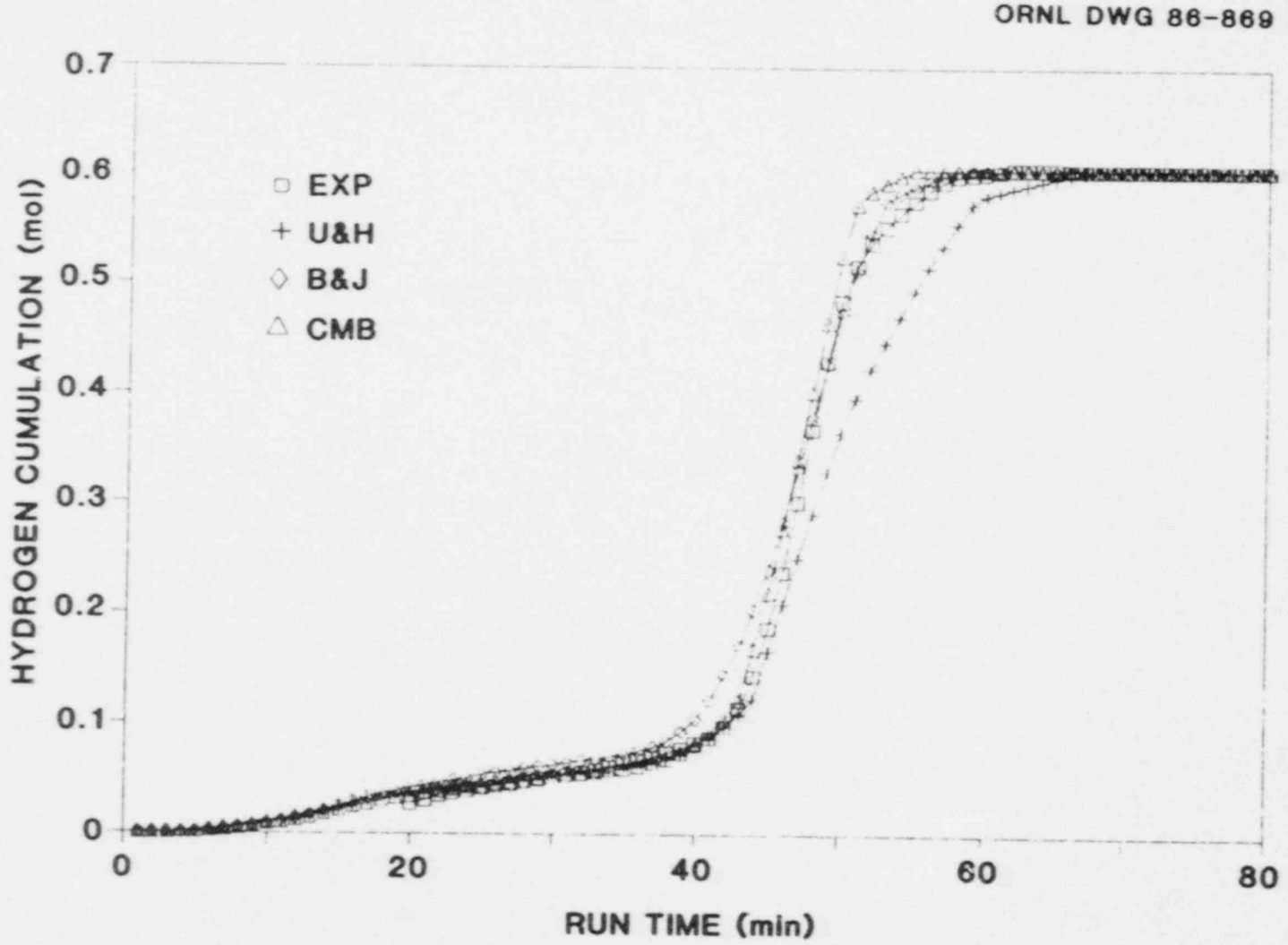

Fig. 14. Comparison of hydrogen accumulation from measured and calculated values for test VT-12.

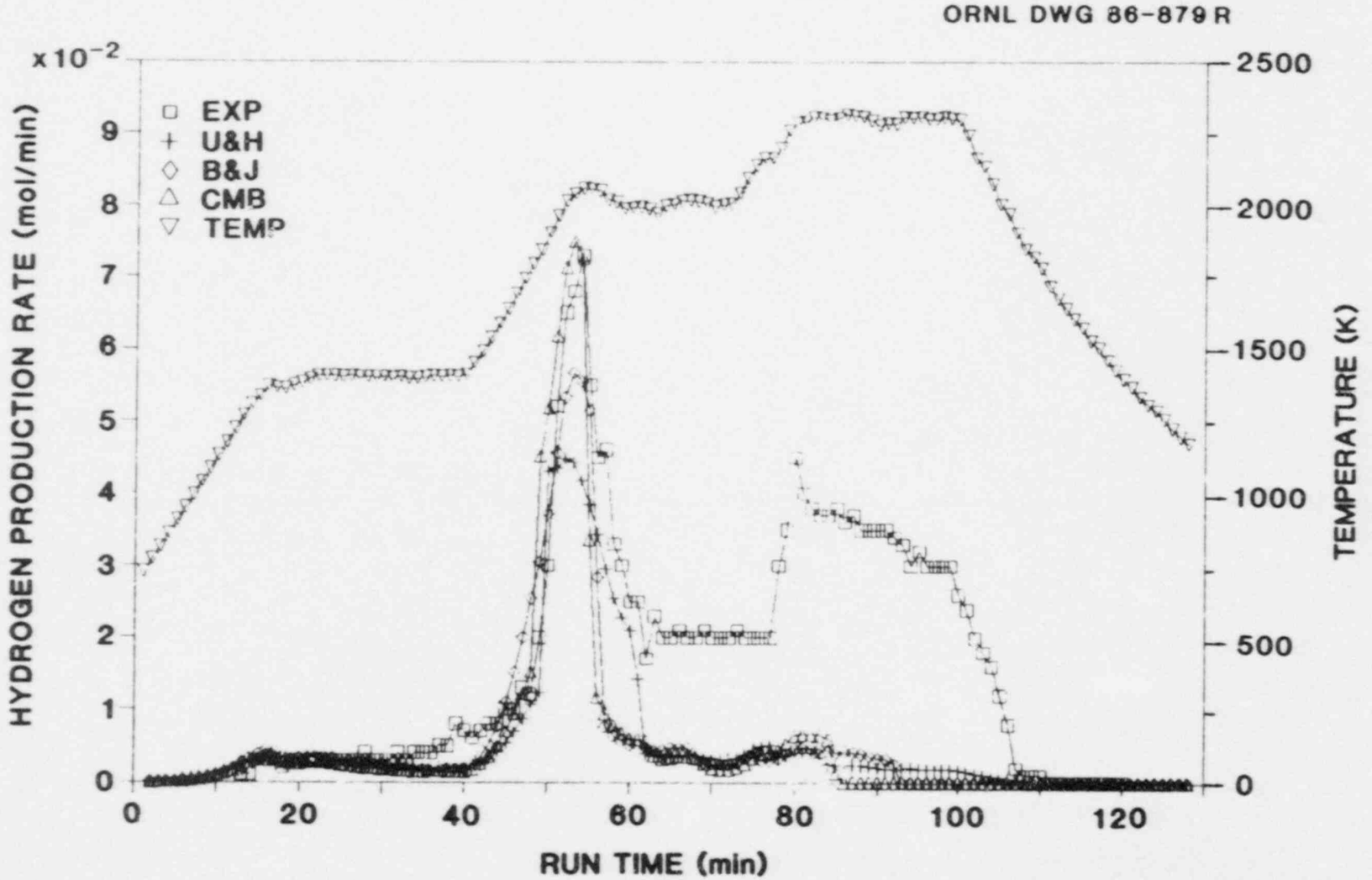

Fig. 15. Comparison of hydrogen production rates from measured and calculated values for test VI-1.

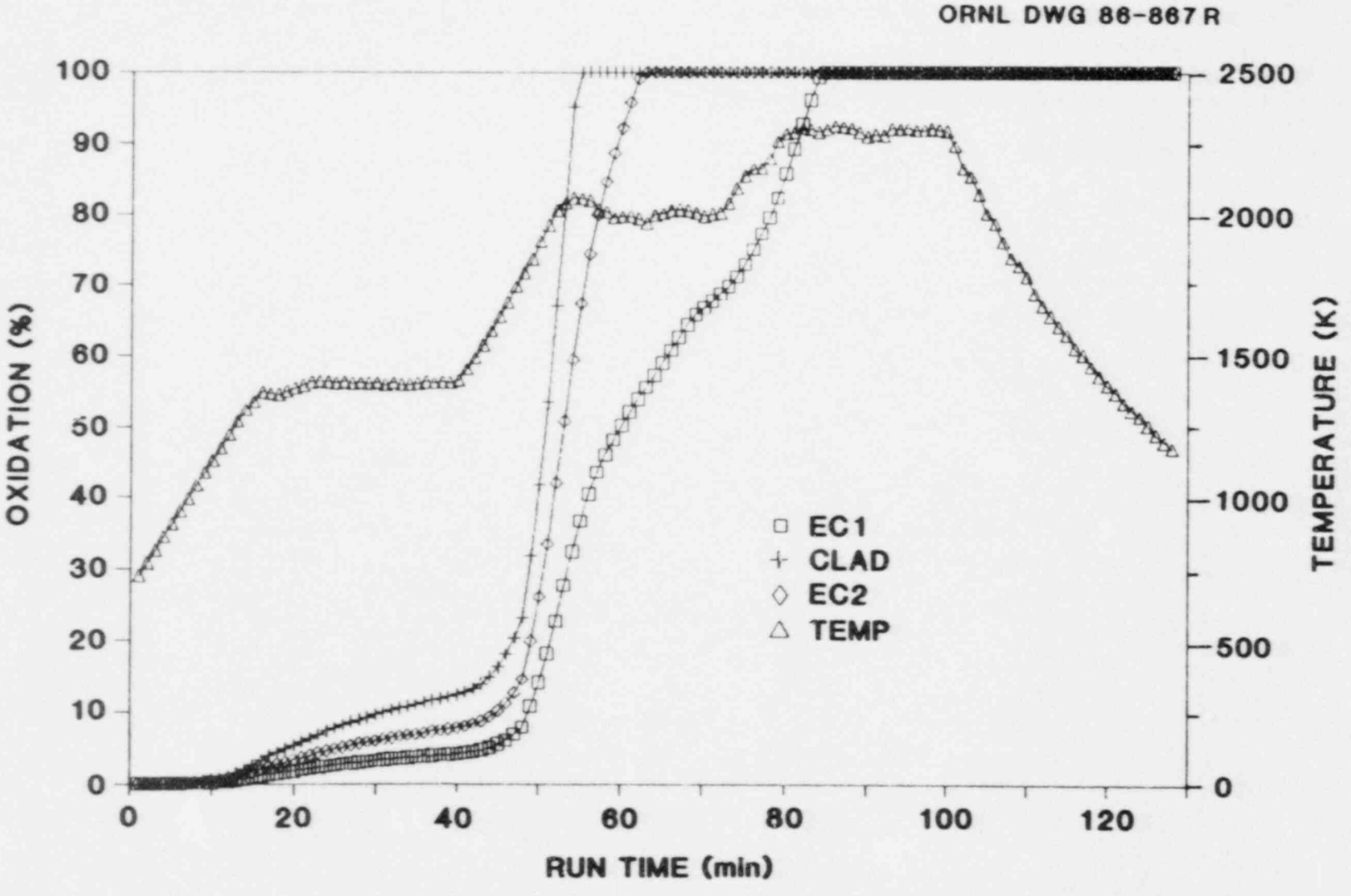

Fig. 16. Calculated cladding oxidation using the PPC data for test VI-1.

run time in Fig. 17. In this estimation, input data for heat release from the Zircaloy oxidation were calculated by using the U&H oxidation rate constant. The curve with the squares shows the temperatures of the zirconia liner and is based on the optical pyrometer measurements. The other curve shows the calculated cladding temperatures. The maximum temperature difference between the curves is ~50 K. After 54 min of run time, the cladding temperature was calculated to reach ~2100 K, which exceeds the melting temperature of unoxidized Zircaloy. However, because the degree of cladding oxidation at that time had reached 95% (Fig. 16), only limited cladding melting could have occurred. Cross sectional photographs of radial sections from test VI-1 fuel were taken and verify that assumption as shown in Fig. 18. These photos show that the cladding tube was completely oxidized and that there was little indication of cladding melting or reaction between the cladding and fuel.

The atmosphere surrounding the fuel specimen varied during test VI-1 and was evaluated from results of the cladding oxidation calculations. The hydrogen concentration $(H_2CONC)_n$, in percent, of the n^{th} period was calculated by the following equation:

$$(H_2CONC)_n = 100(HPR)_n/(SSR) , \qquad (23)$$

where

$(HPR)_n$ = H_2 production rate during the n^{th} period, mol/min,
(SSR) = initial steam supply rate, mol/min.

Since helium in the carrier gas was not involved in the reaction, it was not included in Eq. (23). The variation of hydrogen concentration is shown as the curve with squares as a function of run time in Fig. 19. After 49 min of run time, the hydrogen concentration exceeded 50% and reached 100% after 53 min. However, the period of a high hydrogen concentration lasted only 5 min and for the rest of the test it was <10%.

The oxygen potential of the test atmosphere was calculated by Eq. (24):

$$G_{O_2} = RT\ln(P_{O_2}) \qquad (24)$$

where

P_{O_2} = partial pressure of oxygen, atm,
R = gas constant,
T = absolute temperature.

The oxygen partial pressure of the system is connected with the H_2/H_2O ratio in the atmosphere as:

$$\ln(P_{O_2}) = -2\ \ln(K) - 2\ \ln(P_{H_2}/P_{H_2O}) \qquad (25)$$

where K is the equilibrium constant for the reaction for the formation of water. Figure 20 shows the estimated history of the oxygen potential of

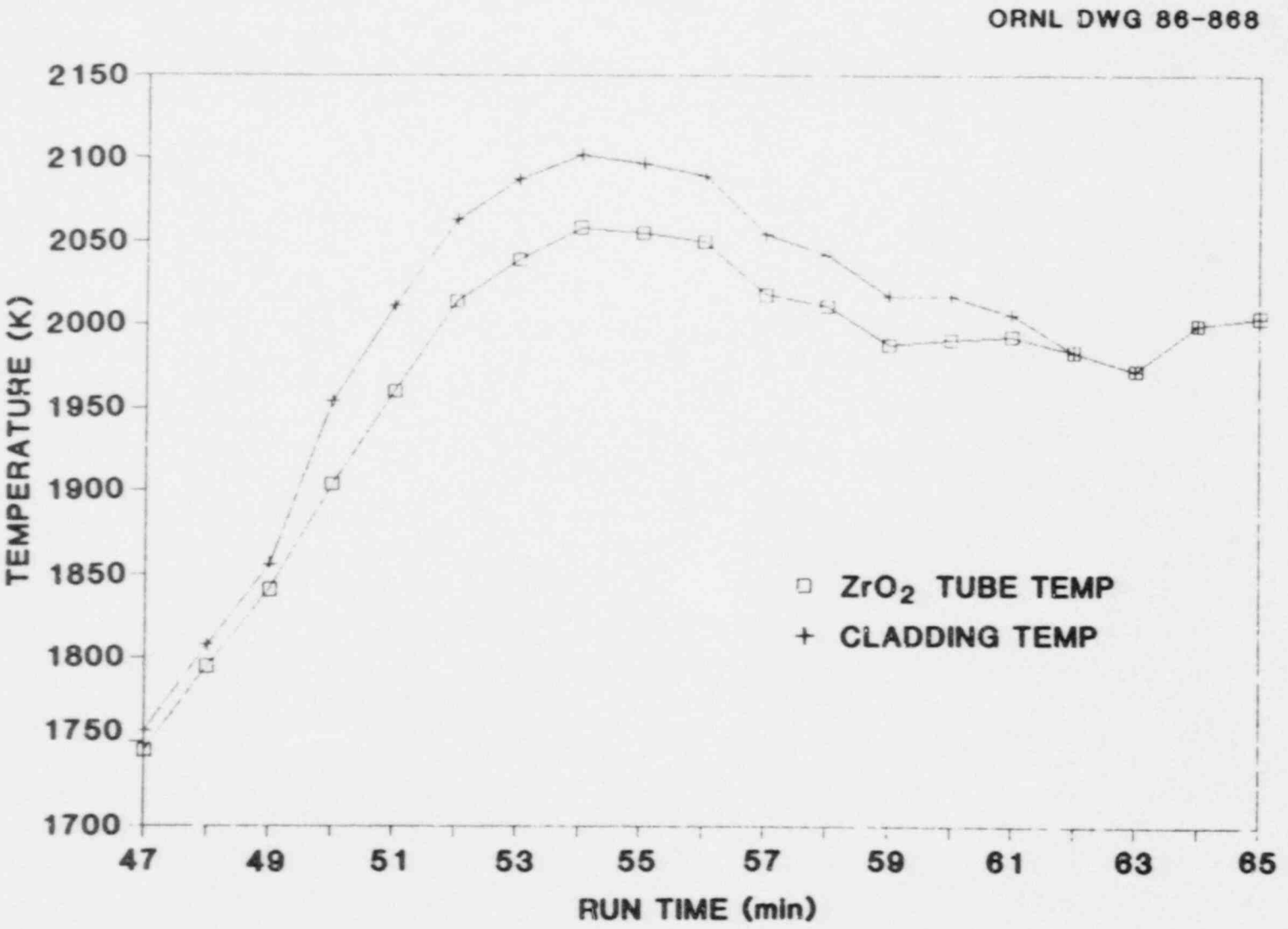

Fig. 17. Temperature difference between the zirconia tube liner and the cladding as calculated by the HEATING6 computer code.

ORNL PHOTO 309-86

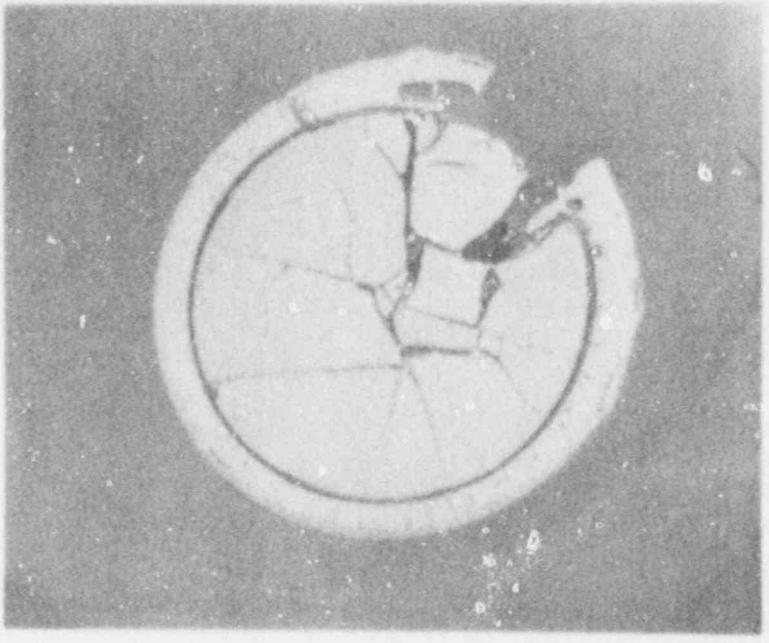

(a)

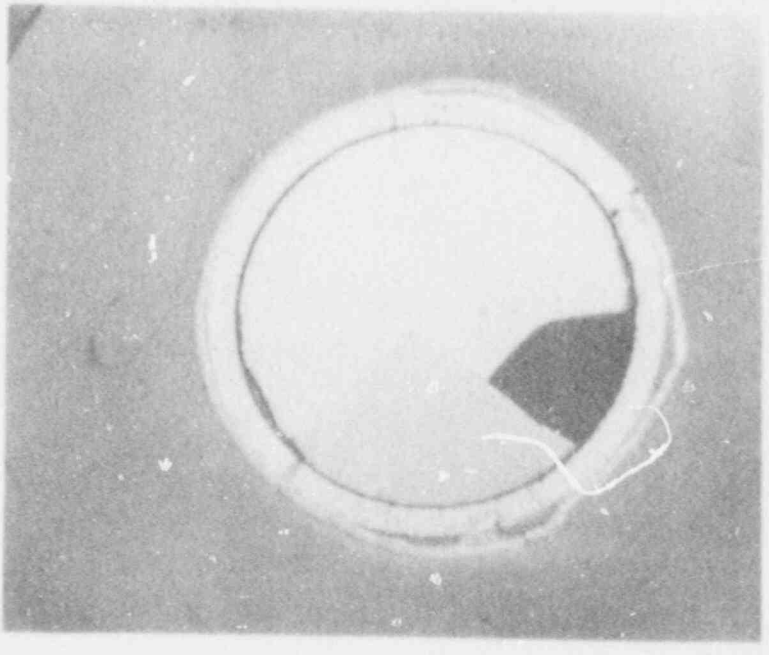

(b)

Fig. 18. Cross-sectional views of test VI-1 fuel specimens. (a) Cross-section at 13 cm from the bottom; (b) cross-section at 5.5 cm from the bottom.

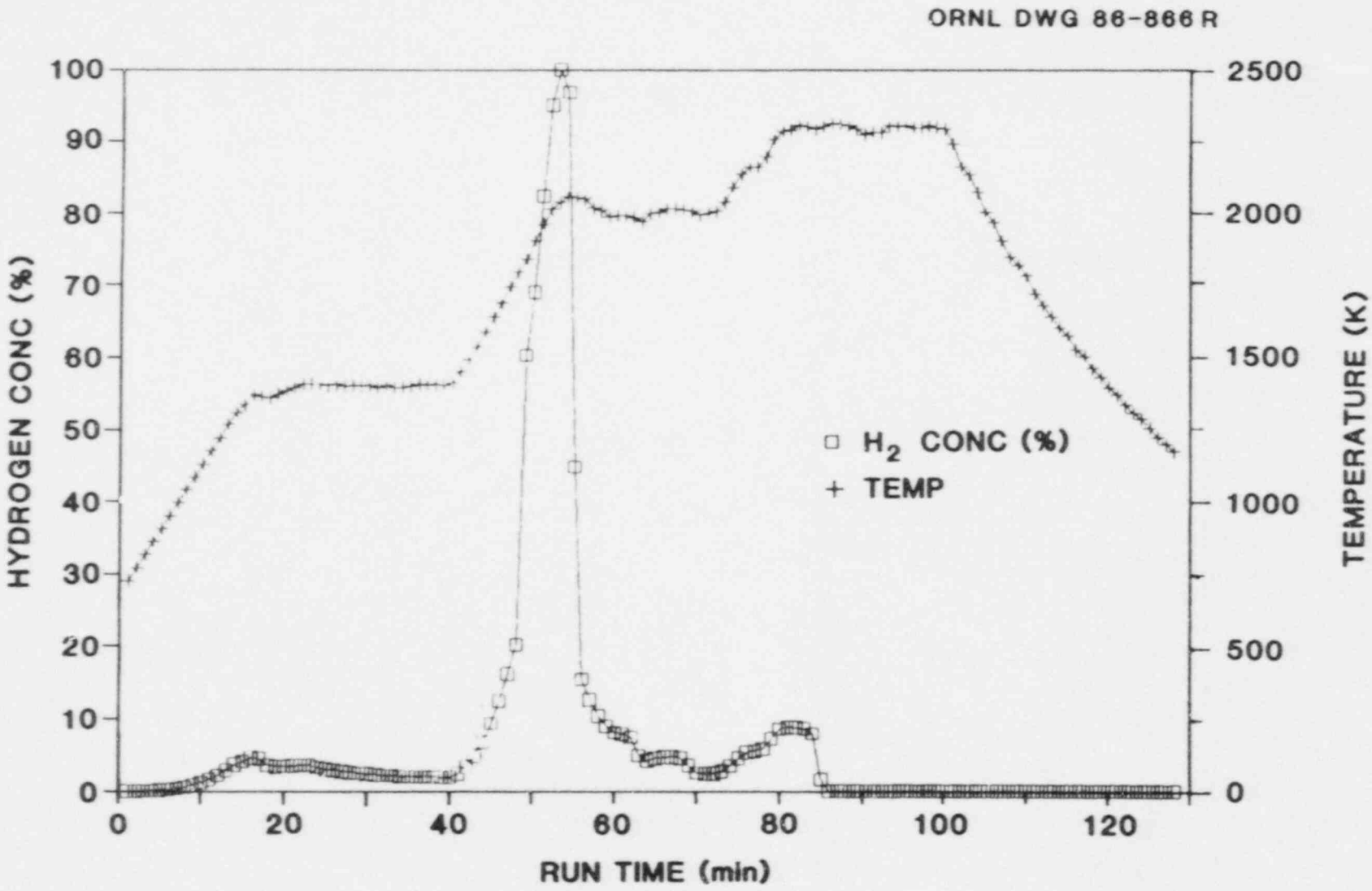

Fig. 19. Variation of hydrogen concentration during test VI-1.

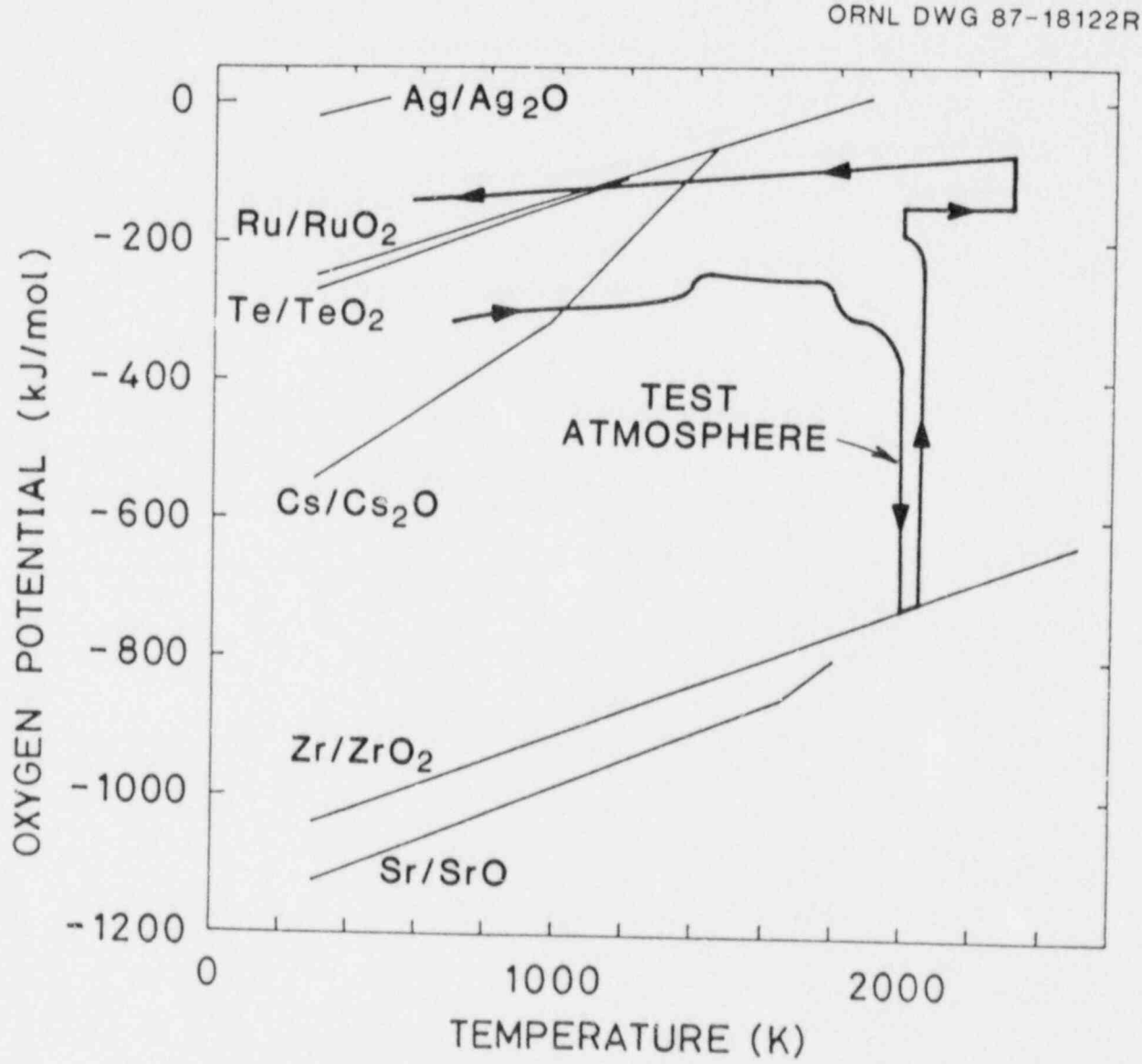

Fig. 20. Oxygen potential of the test VI-1 atmosphere and oxygen potential for typical fission product oxides.

the atmosphere together with the oxygen potential curves for typical fission product oxides.[25,26] The bold line with arrows indicates the oxygen potential of the test atmosphere. The oxygen potential during the heatup to 2000 K was ~ -300 kJ/mol and was low enough to reduce the oxides such as Cs_2O, TeO_2 and RuO_2, but was too high to reduce the so-called refractory oxides such as ZrO_2, SrO and BaO. The oxygen potential during cooldown was ~ -100 kJ/mol — a value comparable to the free energy of formation of Cs_2O, TeO_2 and RuO_2.

6.3 TEST VT-3

The calculated oxidation profile of the cladding and overall oxidation can be compared with the results obtained in test VT-3. Results of the degree of cladding oxidation and overall oxidation are summarized in Table 6. By use of the oxidation rate constant obtained from the PPC

Table 6. Results of cladding oxidation in test VT-3

	Oxidation degree (%)			Overall oxidation (%)
	CL-1	CL-6	CL-11	
Experimental results				
Weight increase	NA[a]	NA	NA	53
CO and H_2O	NA	NA	NA	58
CuO and H_2O	NA	NA	NA	59
NAA[b]	75	44	19	NA
Calculated results				
WOATG[c]	95.1	44.6	26.0	55.7
WATG[d]	92.9	42.2	21.8	53.2

[a] NA = not analyzed.
[b] NAA = neutron activation analysis.
[c] WOATG = without axial thermal gradient.
[d] WATG = with axial thermal gradient.

data, several calculations were carried out to fit the experimental results by changing the values of the steam supply rate and the axial thermal gradient of the cladding. The results that gave the best fit were obtained when the calculations were made using the conditions (1) steam supply rate of 0.55 L/min and (2) the axial temperature change of the fuel specimen as ~75 K. The temperature profile change used in the calculation is shown in Fig. 21. The temperature of each node was determined by subtracting the profile values from the fuel temperature shown by curve A in Fig. 6.

The calculated oxidation profile is plotted in Fig. 22, together with three experimental values which were determined by neutron activation

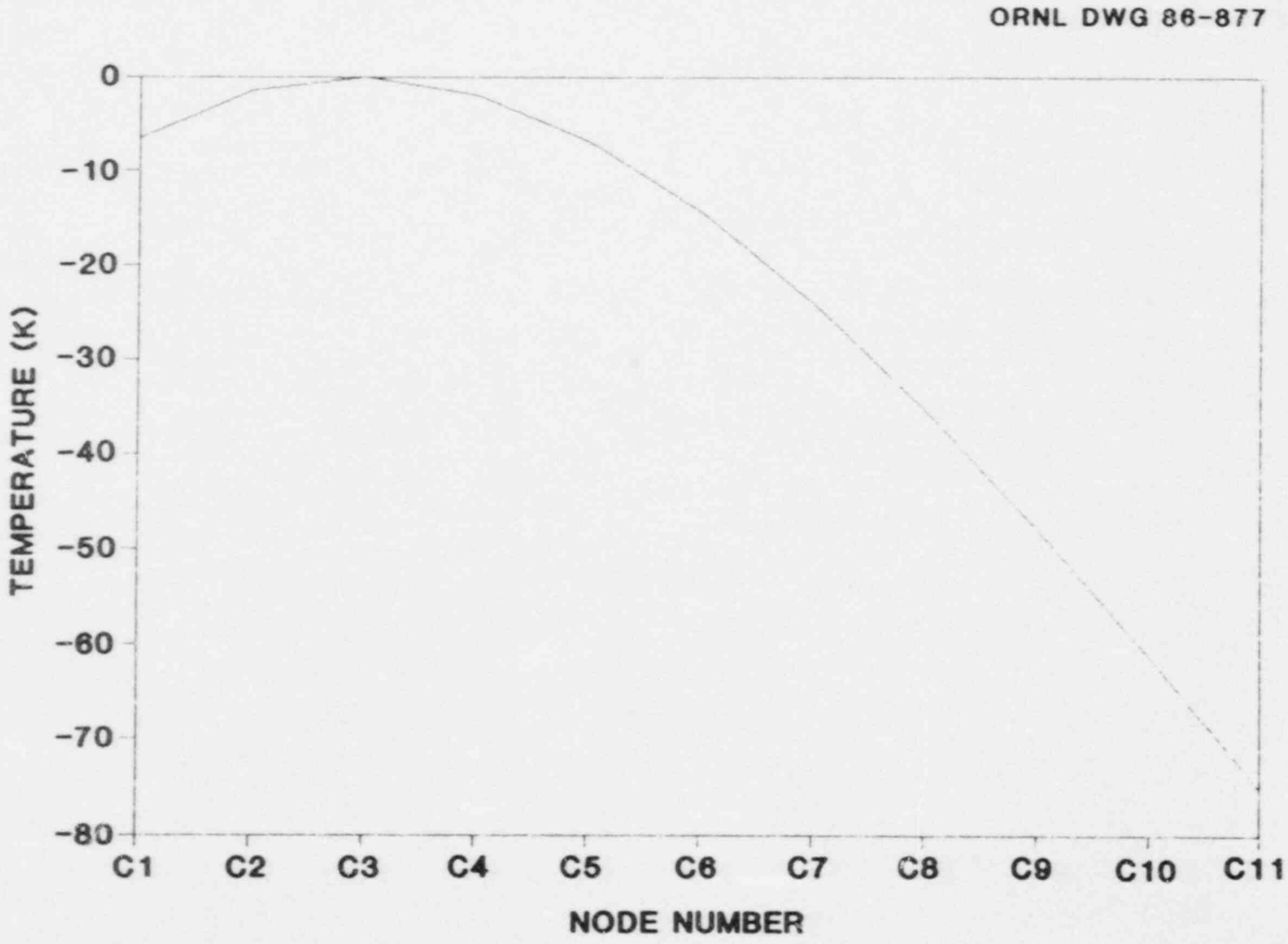

Fig. 21. Axial temperature profile used in the cladding oxidation calculation for test VT-3. Temperature "0" refers to the fuel temperature.

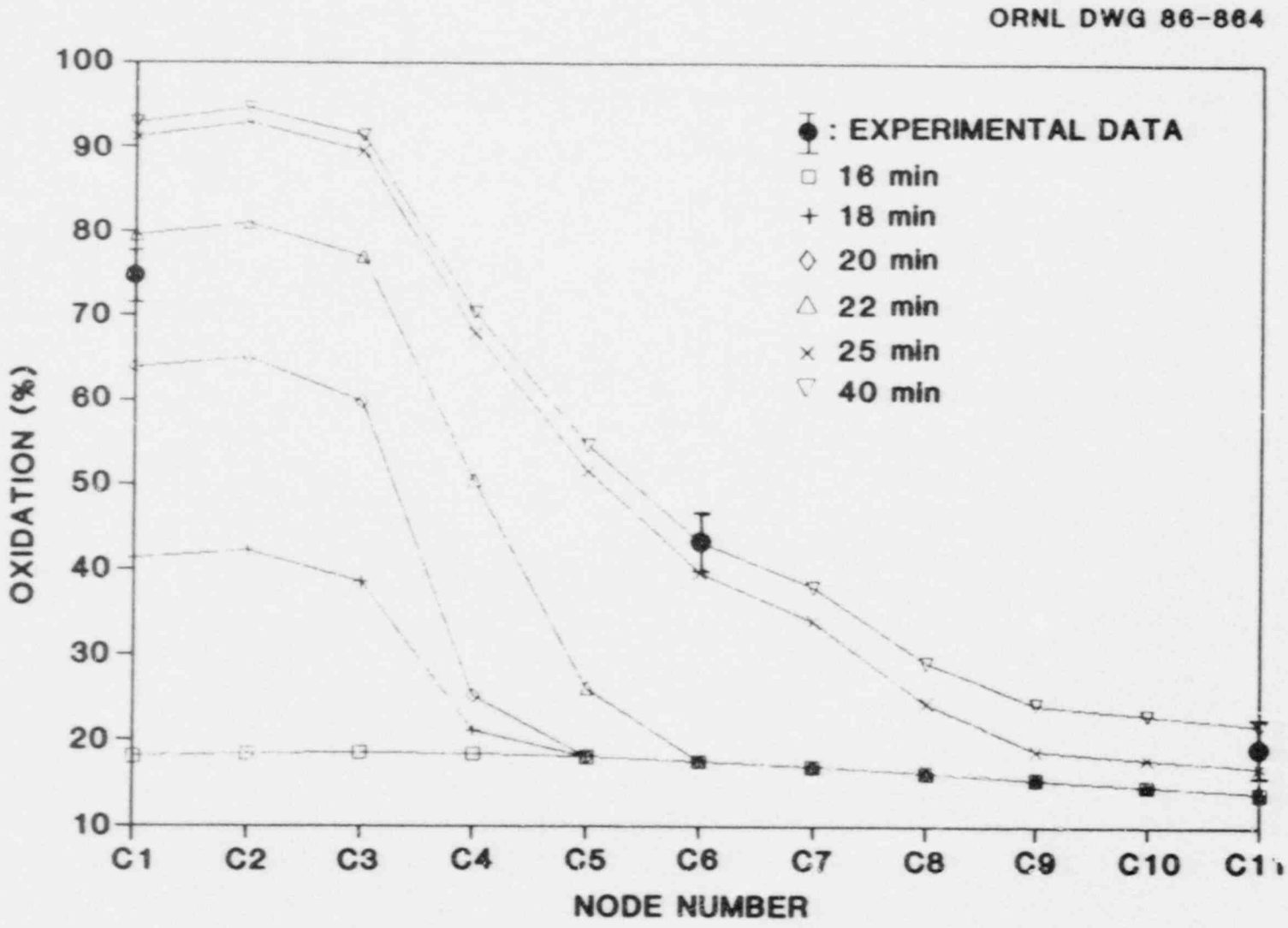

Fig. 22. Calculated oxidation profile for the test VT-3 cladding. Circles show the experimental values.

analysis. The horizontal axis gives the node numbers starting from the upstream end (bottom) of the cladding tube and the vertical axis gives the percent oxidation. Each curve shows the oxidation profile at the run time indicated. For the first 16 min of run time there was slight, but fairly uniform oxidation, along the whole tube. Then, the oxidation rate increased and all the steam was consumed by the upstream half and no steam was available for the downstream half. The curve with downward-triangles shows the final oxidation profile and can be compared with the experimental data indicated by circles. The agreement between them is satisfactory though the oxidation of nodes C-1 through C-3 are higher than the neutron activation value. Figure 23 shows the cross-sectional view of the cladding near the bottom end cap. A gray area in the cladding is the ZrO_2 phase and the white area is the alpha-Zr(O) phase. The figure indicates nearly complete oxidation of Zircaloy cladding.

It is worthwhile to note that not all the steam supplied to the furnace was used to oxidize the cladding tube. In the best fit calculations for this test, the steam supply rate was reduced to 0.55 L/min from the nominal value of 1.2 L/min. This rate means that about half of the steam supplied was by-passed through the susceptor blanket region and reacted with the graphite susceptor to produce additional hydrogen and CO. To be able to evaluate the amount of steam that was available for the cladding oxidation, it was essential to measure the total amounts of hydrogen and CO (or CO_2) generated. Equipment to make these measurements was not in place at the time test VT-3 was run. Changes in the induction heating coil have been made to reduce the axial temperature gradient.

7. CONCLUSIONS

A simple model (ZIRCOX) has been developed to calculate the extent of oxidation of Zircaloy cladding in the vertical furnace tests. Calculated results were tested against the degree of cladding oxidation and hydrogen production that were determined experimentally.

The following findings and conclusions were obtained from the present study:

1. The calculated results represented the experimental data very well.

2. The rate constant for Zircaloy oxidation that gave the best calculated hydrogen production was one based upon the combined data of Pawel et al. and Prater and Courtright. The Urbanic and Heidrick data under-predicted the experiments at temperatures above ~1800 K and the Baker and Just's data over-predicted the Zircaloy/steam reaction in the temperature range between 1300 and 1800 K.

3. The best-fitted profile of cladding oxidation in test VT-3 was obtained under conditions such that the steam supply rate was 0.55 L/min and the axial temperature change was ~75 K.

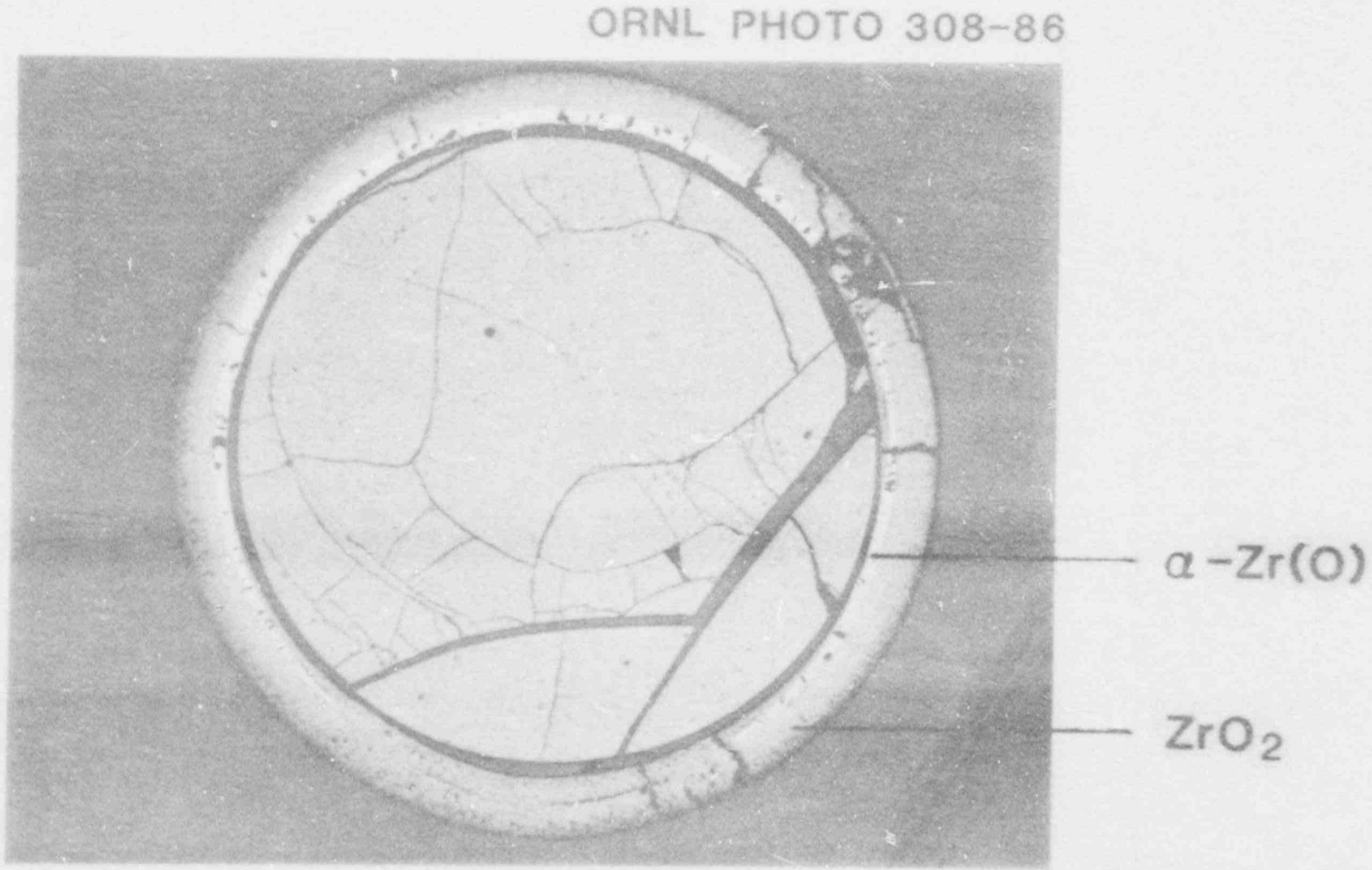

Fig. 23. Cross-sectional view of the test VT-3 fuel specimen near the bottom end cap.

4. The HEATING6 heat transfer computer program showed that the maximum temperature difference between the cladding and the surrounding zirconia furnace tube liner was ~50 K.

5. The atmosphere during test VI-1 was estimated to be fairly rich in steam. For most of the test, the H_2/H_2O ratio was <0.1 except for a short period in the run time between 49 and 54 min when the H_2/H_2O ratio was more than unity.

6. The oxygen potential of the atmosphere during the second and third 20-min periods of test VI-1 was evaluated to be in a range between -100 and -150 kJ/mol, which was low enough to reduce oxides such as Cs_2O, TeO_2 and RuO_2 to their metallic states.

8. ACKNOWLEDGMENTS

The author gratefully acknowledges the significant contributions of several colleagues in conducting this work: M. F. Osborne, R. A. Lorenz, J. L. Collins, J. R. Travis, C. S. Webster, and S. J. Wisbey for performing the cladding oxidation tests and for fruitful discussions; J. C. Mailen, S. D. Clinton, R. E. Pawel, and J. V. Cathcart for technical reviewing; B. C. Drake for preparation of the manuscript; and F. M. Scheitlin for editing.

The author also wishes to thank the Japan Atomic Energy Research Institute, who supported me at ORNL under an administrative agreement with the U. S. Nuclear Regulatory Commission.

9. REFERENCES

1. R. A. Lorenz, J. L. Collins, and S. R. Manning, Fission Product Release from Simulated LWR Fuel, NUREG/CR-0274 (ORNL/NUREG/TM-154), Oak Ridge National Laboratory, October 1978.

2. R. A. Lorenz, J. L. Collins, A. P. Malinauskas, O. L. Kirkland, and R. L. Towns, Fission Product Release from Highly Irradiated LWR Fuel, NUREG/CR-0722 (ORNL/NUREG/TM-287/R2), Oak Ridge National Laboratory, February 1980.

3. R. A. Lorenz, J. L. Collins, and A. P. Malinauskas, Fission Product Source Terms for the LWR Loss-of-Coolant Accident, NUREG/CR-1288 (ORNL/NUREG/TM-321), Oak Ridge National Laboratory, August 1980.

4. R. A. Lorenz, J. L. Collins, A. P. Malinauskas, M. F. Osborne, and R. L. Towns, Fission Product Release from Highly Irradiated LWR Fuel Heated to 1300-1600°C in Steam, NUREG/CR-1386 (ORNL/NUREG/TM-346), Oak Ridge National Laboratory, November 1980.

5. R. A. Lorenz, J. L. Collins, M. F. Osborne, R. L. Towns, and A. P. Malinauskas, Fission Product Release from BWR Fuel Under LOCA Conditions, NUREG/CR-1773 (ORNL/NUREG/TM-388), Oak Ridge National Laboratory, July 1981.

6. M. F. Osborne, R. A. Lorenz, J. R. Travis, and C. S. Webster, Data Summary Report for Fission Product Release Test HI-1, NUREG/CR-2928 (ORNL/TM-8500), Oak Ridge National Laboratory, December 1982.

7. M. F. Osborne, R. A. Lorenz, J. R. Travis, C. S. Webster, and K. S. Norwood, Data Summary Report for Fission Product Release Test HI-2, NUREG/CR-3171 (ORNL/TM-8667), Oak Ridge National Laboratory, February 1984.

8. M. F. Osborne, R. A. Lorenz, K. S. Norwood, J. R. Travis, and C. S. Webster, Data Summary Report for Fission Product Release Test HI-3, NUREG/CR-3335 (ORNL/TM-8793), Oak Ridge National Laboratory, April 1984.

9. M. F. Osborne, J. L. Collins, R. A. Lorenz, K. S. Norwood, J. R. Travis, and C. S. Webster, Data Summary Report for Fission Product Release Test HI-4, NUREG/CR-3600 (ORNL/TM-9001), Oak Ridge National Laboratory, June 1984.

10. M. F. Osborne, J. L. Collins, R. A. Lorenz, K. S. Norwood, J. R. Travis, and C. S. Webster, Data Summary Report for Fission Product Release Test HI-5, NUREG/CR-4037 (ORNL/TM-9437), Oak Ridge National Laboratory, June 1985.

11. M. F. Osborne, J. L. Collins, R. A. Lorenz, K. S. Norwood, J. R. Travis, and C. S. Webster, Data Summary Report for Fission Product Release Test HI-6, NUREG/CR-4043 (ORNL/TM-9433), Oak Ridge National Laboratory, September 1985.

12. M. F. Osborne, J. L. Collins, R. A. Lorenz, J. R. Travis and C. S. Webster, Design and Final Safety Analysis Report for Vertical Fission Product Release Apparatus in Hot Cell B, Building 4501, NUREG/CR-4332 (ORNL/TM-9720), Oak Ridge National Laboratory, March 1986.

13. H. Etherington, Ed., Nuclear Engineering Handbook, 1st ed., McGraw-Hill, New York, 1958.

14. L. Baker and L. C. Just, ANL-6548, 1962.

15. V. F. Urbanic and T. R. Heidrick, J. Nucl. Mater. 75, 251 (1978).

16. R. E. Pawel, J. V. Cathcart and R. A. McKee, J. Electrochem. Soc. 126, 1105 (1979).

17. S. Malang, SIMTRAN-I, A Computer Code for the Simultaneous Calculation of Oxygen Distributions and Temperature Profiles in Zircaloy During Exposure to High-Temperature Oxidizing Environments, ORNL-5083, Oak Ridge National Laboratory, November 1975.

18. H. J. Neitzel, "PECLOX MODEL, Modeling of the Chemical Pellet-Cladding-Interaction and/or Zircaloy-Steam-Oxidation under Severe Damage Conditions," The Semi-Annual SFD Review Meeting, Albuquerque, New Mexico, April 9-11, 1984.

19. H. Uetsuka, P. Hofmann, J. Burbach, and H. Metzger, Reaction Kinetics of Zircaloy-4 in a 25% O_2/75% Ar Gas Mixture from 900 to 1500°C under Isothermal Conditions, KfK-3917, 1983.

20. J. T. Prater and E. L. Courtright, High-Temperature Oxidation of Zircaloy-4 in Steam and Steam-Hydrogen Environments, NUREG/CR-4476 (PNL-5558), Pacific Northwest Laboratories, February 1986.

21. J. T. Prater and E. L. Courtright, private communication, April 1986.

22. R. A. Lorenz, private communication, December 1985.

23. D. C. Elrod et al., HEATING6: A Multidimensional Heat Conduction Analysis with the Finite-Difference Formulation, ORNL/NUREG/CSD-2/V2, Oak Ridge National Laboratory, October 1981.

24. O. Kubaschewski and C. B. Alcock, Metallurgical Thermochemistry, 5th ed., Pergamon Press, New York, 1979.

25. R. Stull and H. Prophet, eds., JANAF Thermochemical Tables, 2nd ed. U.S. Government Printing Office, Washington D.C., 1971.

26. L. B. Pankratz, Thermodynamic Properties of Elements and Oxides, Bulletin: 672, U.S. Government Printing Office, Washington D.C., 1982.

NUREG/CR-4777
ORNL/TM-10272
Dist. Category R3

INTERNAL DISTRIBUTION

1. E. C. Beahm
2. J. T. Bell
3. S. D. Clinton
4-7. J. L. Collins
8. S. R. Daish
9. C. W. Forsberg
10. R. W. Glass
11. J. R. Hightower
12. S. A. Hodge
13. E. K. Johnson
14. T. S. Kress
15. T. B. Lindemer
16. H. K. Lee
17-21. R. A. Lorenz
22. T. Nakamura
23-27. M. F. Osborne
28. R. E. Pawel
29. F. M. Scheitlin
30. M. G. Stewart
31. Y.-C. Tong
32. J. R. Travis
33. C. S. Webster
34. J. H. Wilson
35. A. L. Wright
36. R. G. Wymer
37. Central Research Library
38. ORNL-Y-12 Technical Library Document Reference Section
39. Laboratory Records
40. Laboratory Records, ORNL RC
41. ORNL Patent Section

EXTERNAL DISTRIBUTION

42. Office of Assistant Manager for Energy Research and Development, ORO-DOE, P.O. Box E, Oak Ridge, TN 37831
43. Director, Division of Reactor Safety Research, U.S. Nuclear Regulatory Commission, Washington, DC 20555
44-45. Technical Information Center, DOE, Oak Ridge, TN 37981
46. Division of Technical Information and Document Control, U.S. Nuclear Regulatory Commission, Washington, DC 20555
47. L. K. Chan, Accident Evaluation Branch, U.S. Nuclear Regulatory Commission, 5650 Nicholson Lane, Rockville, MD 20852
48. R. O. Meyer, Accident Evaluation Branch, U.S. Nuclear Regulatory Commission, 5650 Nicholson Lane, Rockville, MD 20852
49. J. A. Mitchell, Accident Evaluation Branch, U.S. Nuclear Regulatory Commission, 5650 Nicholson Lane, Rockville, MD 20852
50. M. Silberberg, Accident Evaluation Branch, U.S. Nuclear Regulatory Commission, 5650 Nicholson Lane, Rockville, MD 20852
51-300. Given distribution as shown in Category R3 (NTIS – 10)

NRC FORM 335 (2-84) NRCM 1102 3201, 3202

U.S. NUCLEAR REGULATORY COMMISSION

BIBLIOGRAPHIC DATA SHEET

SEE INSTRUCTIONS ON THE REVERSE

1 REPORT NUMBER (Assigned by TIDC and Vol. No., if any)

NUREG/CR-4777
ORNL/TM-10272

2 TITLE AND SUBTITLE

Steam Oxidation of Zircaloy Cladding in the ORNL Fission Product Release Tests

3 LEAVE BLANK

4 DATE REPORT COMPLETED

MONTH	YEAR
February	1987

5 AUTHOR(S)

Toshiyuki Yamashita

6 DATE REPORT ISSUED

MONTH	YEAR
March	1988

7 PERFORMING ORGANIZATION NAME AND MAILING ADDRESS (Include Zip Code)

Oak Ridge National Laboratory
P.O. Box X
Oak Ridge, TN 37831

8 PROJECT/TASK/WORK UNIT NUMBER

9 FIN OR GRANT NUMBER

B0127

10 SPONSORING ORGANIZATION NAME AND MAILING ADDRESS (Include Zip Code)

U.S. Nuclear Regulatory Commission
Accident Evaluation Branch
Division of Reactor System Safety
Washington, DC 20555

11a TYPE OF REPORT

NUREG

b PERIOD COVERED (Inclusive dates)

12 SUPPLEMENTARY NOTES

13 ABSTRACT (200 words or less)

A simple model (ZIRCOX) has been developed to calculate the extent of oxidation of Zircaloy cladding in the vertical furnace tests conducted at ORNL. The model is based on the fact that the oxidation of Zircaloy is governed by the parabolic rate law. By introducing the equivalent time t', the model is able to handle nonisothermal oxidation as well as isothermal.

The degree of cladding oxidation and H_2 production were calculated using three sets of rate constants for the Zircaloy oxidation, and these results were compared with those measured experimentally. The calculated results showed excellent agreement with the experiments. The rate constant for Zircaloy oxidation that gave the best agreement was one based upon combined Pawel et al. and Prater and Courtright data.

The temperature difference between the cladding and the zirconia furnace tube liner was estimated by the HEATING6 heat transfer program and was found to be ~50 K for the maximum oxidation rate.

The heating atmosphere during test VI-1 was also evaluated in terms of the oxygen potential.

14 DOCUMENT ANALYSIS - a KEYWORDS/DESCRIPTORS

Steam Oxidation, Hydrogen Production, Zircaloy Cladding, Model, Rates

b IDENTIFIERS/OPEN-ENDED TERMS

15 AVAILABILITY STATEMENT

NTIS

16 SECURITY CLASSIFICATION

(This page)
Unclassified

(This report)
Unclassified

17 NUMBER OF PAGES

45

18 PRICE

☆U.S. GOVERNMENT PRINTING OFFICE 1988-548-118/60199

120555078877 1 1AN1R3
US NRC-OARM-ADM
DIV OF PUB SVCS
POLICY & PUB MGT BR-PDR NUREG
W-537
WASHINGTON DC 20555